Design of a Small Vacuum Facility for Microflow Experiments

A Major Qualifying Project Report

Submitted to the Faculty

of the

WORCESTER POLYTECHNIC INSTITUTE

in partial fulfillment of the requirements for the

Degree of Bachelor of Science

in Mechanical Engineering

by

Jairo Argueta Dimitrios Bakllas Elias Karam

Samantha Millar David Wiig

Date: March 5th, 2010

Approved:

Professor Nikolaos A. Gatsonis, MQP Advisor

Abstract

The project considers the integration of an automated hoist system with the support table of the Small Vacuum Facility (SVF). The procured free-standing hoist can lift the 114-kg bell-jar cover and clear 76 cm from the support table. Design iterations using structural analysis software determine the optimal position of the hoist, the design of integration components, and the structural impact on the support table. Fabrication of parts and integration is pursued with commercial vendors. The project involves also the estimation of mass flow rates for free-molecular and continuum flows through 0.1–100 micron-diameter orifices into the 10^{-3}–10^{-9} Torr bell-jar. The results are coupled with throughput analysis of the SVF's diffusion pump to establish the feasibility of planned microflow experiments.

Table of Contents

Table of Figures **5**

List of Tables **7**

1 – Introduction **8**

1.1 – Overview **8**

1.2 – Review of Previous Work **10**

1.2.1 – Support Structure of the SVF 10

1.2.2 Microfluid Analysis 14

1.3 – Objectives and Approach **14**

2 – Mechanical Design **17**

2.1 – Hoist Design **17**

2.1.1 – Research on Available Products 18

2.1.2 – Hoist Purchased 20

2.2 Design Iterations **20**

2.2.1 – Hoist Position 21

2.3 – Attachment Bracket **24**

2.4 – Structural Analysis **25**

3 – Microflow Analysis **33**

3.1 – Pumping Operations **33**

3.1.1 – Diffusion Pump Background 33

3.1.2 – Basic Pump Theory 37

3.2 – Flow Through an Orifice **38**

3.2.1 – Continuum Regime 39

3.2.2 – Rarefied Regime 42

3.3 – Tube Flow **45**

3.3.1 – Continuum Regime 45

3.3.2 – Rarefied Regime 46

3.4 – Calculation of Max $\boldsymbol{Mout}$ **47**

4 – Summary and Recommendations **52**

References **54**

Appendix A: Flow Calculator Excel Program **56**

Appendix B: Excel Mass Flow Program..... 57

Appendix C: MATLAB Program (Created by MQP Team)..... 58

Appendix D: MATLAB Code (Created by Michael Morin)..... 60

Table of Figures

Figure 1: Small Vacuum Facility Schematic 9
Figure 2: Flow Delivery System Inside the Test Chamber (Chamberlin, 2007) 9
Figure 3: Support Structure of SVF with Casters and Base Well 11
Figure 4: Heavy Duty Casters 11
Figure 5: Base Well 12
Figure 6: Last Year's Hoist System 12
Figure 7: Final Structure with all Supports 13
Figure 8: Final Structure Displacement Analysis 13
Figure 9: Kurt J. Lesker Company Hoist System 18
Figure 10: WPI Vacuum Facility Hoist System 19
Figure 11: Key High Hoist System 19
Figure 12: Key High Hoist Purchased 20
Figure 13: Hoist System on the Structure Table 21
Figure 14: First Iteration of Hoist Base 21
Figure 15: Second Iteration of Hoist Base 22
Figure 16: Gate Valve 23
Figure 17: Third Iteration of Hoist Base 23
Figure 18: U-Bracket and Side Bracket 24
Figure 19: Stresses on the Whole Structure 25
Figure 20: Deformation on the Whole Structure 26
Figure 21: Von Mises Stresses and Deformation of the Support Bracket 27
Figure 22: Deformation of the Support Bracket 28
Figure 23: Von Mises Stresses one of the Support Bracket Screw 29
Figure 24: Deformation on one of the support bracket screw 30
Figure 25: Von Mises Stresses on One of the Bottom Screws 31
Figure 26: Total Deformation on one of the Bottom Screws 32
Figure 27: Schematic of Vacuum System (Varian, 1992) 34
Figure 28: Diffusion Pump Schematic (Varian, 1992) 34
Figure 29: Mechanical Pump (Varian, 1992) 35
Figure 30: Reservoir Approximation for Orifice Theory 39
Figure 31: Kinetic Effusion Through an Orifice 42
Figure 32: Impact Cylinder Demonstrating the Path of the Escaping Molecules (Gambosi, 1994) 43

Figure 33: Speed Curve for Varian VHS-6 Diffusion Pump (VarianInc.com)..... 48
Figure 34: Speed Curve for DS602 3Ph Dual Stage Rotary Vane (Mechanical) Pump 48
Figure 35: Mass Flow Rate versus P_r with P_b 1.0 X 10^{-3} Torr 50
Figure 36: Mass Flow Rate versus P_r with P_b 5.0 X 10^{-9} Torr 51

List of Tables

Table 1: Deformation Based on Bell Jar Height 27
Table 2: DS602 Mechanical Pump Specifications (Varian, 1992) 36
Table 3: Reservoir and Background Chamber Testing Condition 49
Table 4: Mass Flow Conversion Calculator 49

1 – Introduction

1.1 – Overview

The relevance of microfluid dynamics has substantially increased with the emergence of microfluidic devices in fields such as molecular biology and micro-propulsion. Microfluidics studies the behavior and manipulation of fluids in micron (μ) and smaller scales. Fluid flow at these scales inherently differs from conventional fluid dynamics in that factors such as surface tension and fluidic resistance start to dominate the system. A particular difference among micro and macro flows is an evident decrease in Reynolds number.

Practical applications that take advantage of the design of systems which utilize such small volumes of fluids include spacecraft propulsion used for orbital insertion, station keeping and attitude control of micro, nano and pico satellites. Research at WPI led by the Aerospace Engineering Program has taken an interest in studying the fluid mechanics of such scales by pursuing theoretical, computational, and experimental investigations of gases through microchannels. (Chamberlin and Gatsonis, 2006; Heller and Padden, et al, 2006; Chamberlin and Gatsonis, 2008; Herrera et al, 2008) In order to carry out this research, experiments are planned for a Small Vacuum Facility (SVF) currently under development in HL314. The focus of this Major Qualifying Project (MQP) is to facilitate the integration of such facility by completing design requirements and performing microflow analysis that will support future microfluidic experiments. This MQP expands on the design and fluid analysis initiated by Del Vecchio and Loomis (2009).

A schematic in Figure 1 highlights the most important components of the SVF. When the vacuum facility is operating, the experiments will take place inside the bell jar shown in the insert. The schematic in Figure 2 provides details of the planned experiments, showing a micropitot probe measuring a microjet. (Chamberlin and Gatsonis, 2006; Chamberlin, 2007)

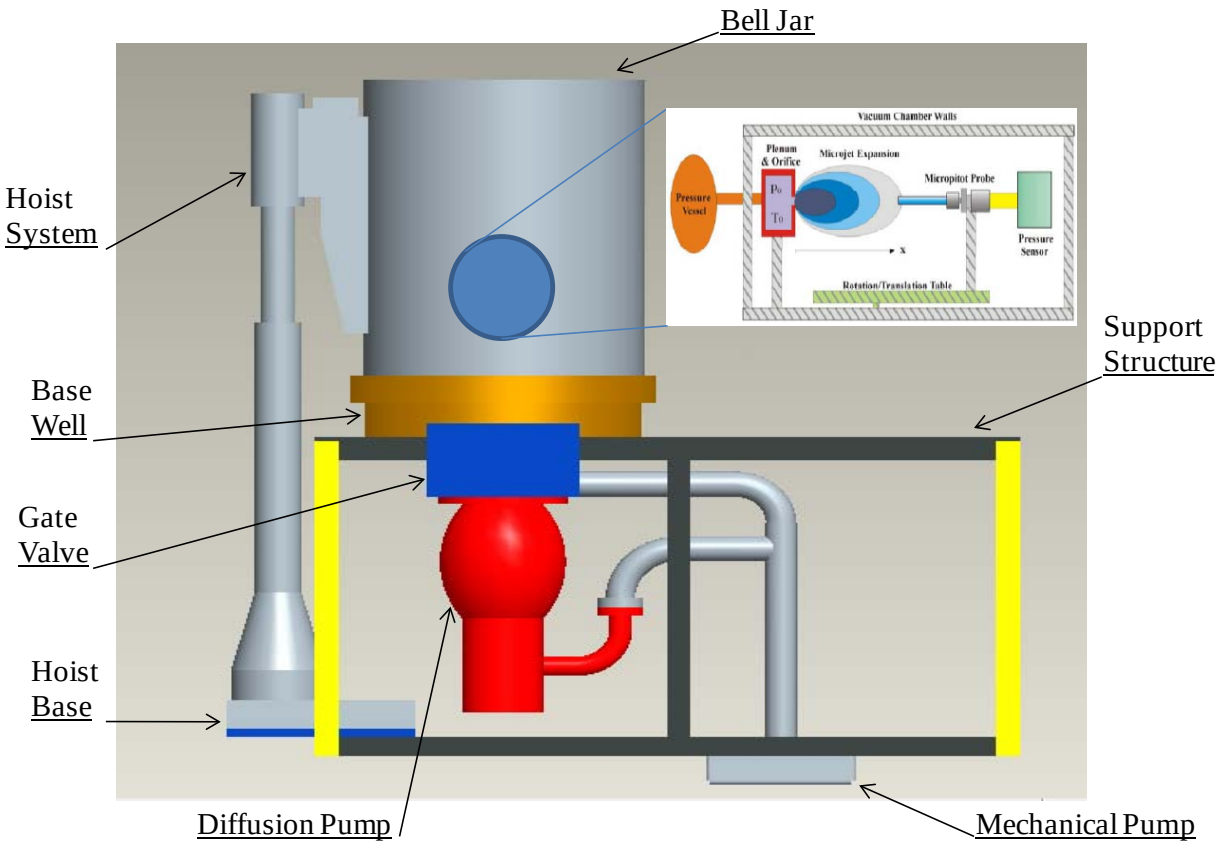

Figure 1: Small Vacuum Facility Schematic

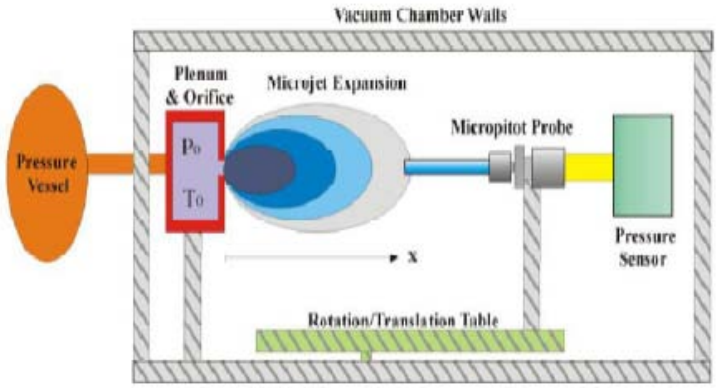

Figure 2: Flow Delivery System Inside the Test Chamber (Chamberlin, 2007)

The project goals are to:

1. Integrate an automated hoist system with the support table of the SVF shown in Figure 1. The free-standing hoist system must be capable of lifting the 114-kg bell-jar cover and clearing 30in from the support table. Iterations using structural analysis software must determine the optimal position of the hoist, the design of the integration components, as well as the structural impact on the support table.

2. Estimate mass flow rates of free-molecular and continuum flows through a 0.1 – 100 micron-diameter orifice into the 10^{-3} – 10^{-9} Torr bell-jar and perform a throughput analysis of the SVF's diffusion pump in order to establish the feasibility of planned microflow experiments.

1.2 – Review of Previous Work

1.2.1 – Support Structure of the SVF

The design and fabrication of the SVF is described by DelVecchio and Loomis (MQP, 2009). In this section, an overview of existing parts and equipment is outlined. The design requirements outlined in last year's MQP are:

- The support structure must hold a total of 544kg (1200lbs). This is the total weight of the bell jar, base well, hoist, diffusion pump, gate valve, experiments and the miscellaneous computers and equipment. This includes the bell jar at 114kg (250lbs), the base well at 108kg (237lbs), the diffusion pump at 34kg (75lbs), the gate valve at 9.07kg (20lbs), the experiment at 91kg (200lbs), the hoist at 64kg (141lbs), and any needed computers or equipment.
- The surface of the support structure must have a hole large enough to accommodate the 0.2794m (11in) diameter base well.
- The surface of the support structure must be large enough to accommodate the 0.6096m (24in) diameter bell jar, equipment, and hoist system.
- The height must be such to fit associated pumps and plumbing underneath it.
- The support structure must be mobile and have the ability to level itself.
- The support structure should have a safety factor of 2 or more in terms of yield stress.
- The support structure should not deflect more than 1mm (0.0394in) uniformly around the hole.

Figure 3: Support Structure of SVF with Casters and Base Well

The support structure of the SVF shown in Figure 3 is partially assembled with the casters attached at the four corners and the base well in place. A manually operated hoist is also attached to the structure.

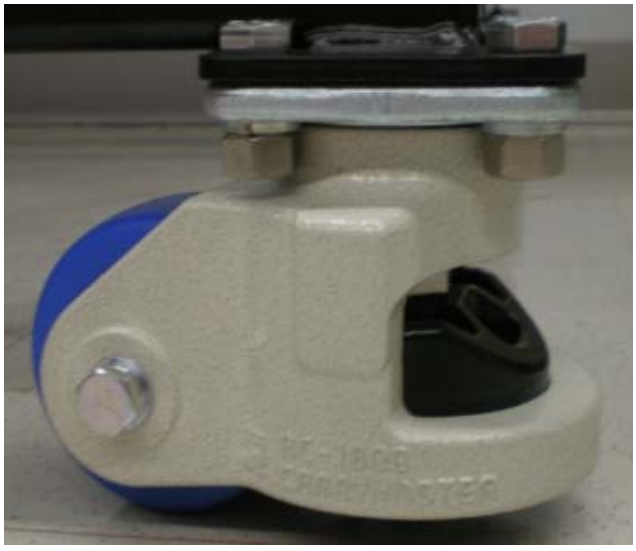

Figure 4: Heavy Duty Casters

The caster shown in Figure 4 is a heavy duty leveling caster with a load capacity of 816.5kg (1800 lbs) per caster. It has a ball bearing setup which allows the user to lower a foot independently at

each of the four corners of the support structure. They provide mobility to the table as well as the ability to level the surface of the structure for experiments to be conducted on a level plane.

Figure 5: Base Well

The base well in Figure 5 has already been integrated to the structure. It has a net weight of 108kg (237 lbs), an outer diameter of 66.04cm (26 inches) and a lower port diameter of 27.94cm (11 inches). It has a total of 18 input ports to facilitate the set up of experiments.

Figure 6: Last Year's Hoist System

Figure 6 shows the hoist system that has a net weight of 63.96kg (141lbs) and the ability to lift the bell jar 30 inches from the base well. There are several deficiencies of this hoist system: a) It is difficult to operate since it has a manually operated crank gear. b) it is unstable since it only attaches to the top of the bell jar with a steel wire hook allowing the bell jar to move freely. c) It may damage the base well and disrupt the vacuum seal.

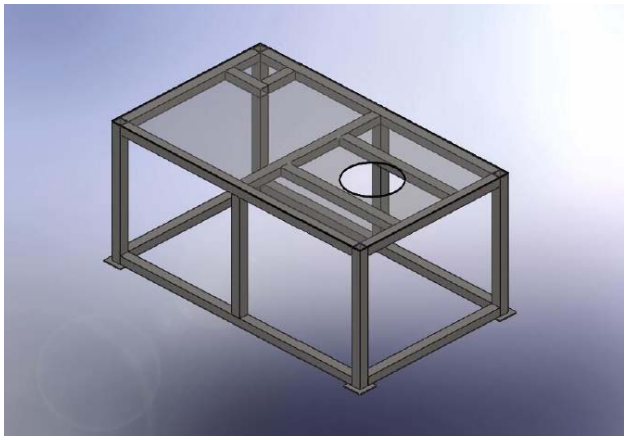

Figure 7: Final Structure with all Supports

Figure 7 illustrates the schematic of the structure designed by DelVecchio and Loomis (2009). To reduce the total deflection around the hole, the top plate is made of A36 steel with a thickness of 0.00635m (0.25 in). There are several beams underneath the top plate in order to support the base well and bell jar weight with minimal deflection. All these supports are important to maintain the maximum displacement of the top surface, which needs to be less than 0.001m (0.0394 in). The experiments that will be conducted in this chamber will be in the microscale; therefore, there cannot be large deflections around the surface.

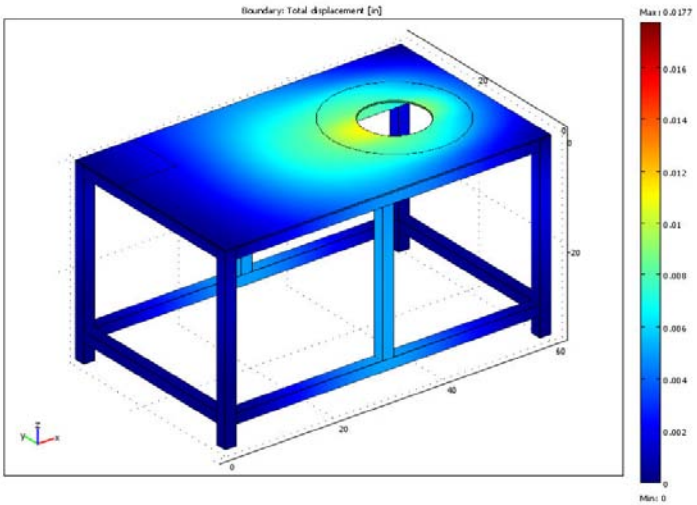

Figure 8: Final Structure Displacement Analysis

The final result of the structural analysis from COMSOL is shown in Figure 8. By assuming a weight of 3336.17N (750 lbs) placed in the annular region around the base well. The maximum deflection of the top surface is 2.79 X 10^{-4}m (0.011 in) and the maximum difference in deflection around the hole is

only 2.5 X 10^{-5}m (0.001 in) which is well within acceptable limits. All design requirements were met for the deflection of the top surface.

1.2.2 Microfluid Analysis

Three previous MQPs carried out research and work that was closely related to the goals of this MQP: "A Microscale Mass-Flow Measuring System" by Heller and Padden (2006), "Integration of a Small Vacuum Facility" by Herrera et al. (2008), and "A Vacuum Facility for Microflow Experiments" by Del Vecchio and Loomis (2009). These MQPs are reviewed below.

Heller and Padden (2006) designed an experimental setup for measuring mass-flow rates as small as 10^{-13} kg/s using a pressure-decay method. Predictions of mass flow rates from microscale orifices were compared to experimental results. Herrera et al. (2008) and Del Vecchio and Loomis (2009) completed a review of microfluid dynamics that is the most relevant to this project. Herrera et al. (2008) covered basic microflow principles and predicted flow behaviors with a previously developed MATLAB code and FLUENT simulations. Del Vecchio and Loomis (2009) presented the theory of flows through micro-orifices for relevant flow regimes and presented MATLAB code predictions.

Our review identified the analysis required to thoroughly cover the fluid regimes and flow characteristics that are expected in the SVF.

1.3 – Objectives and Approach

An overview of the objectives, design requirements and approach are presented below.

1. Design of an Automated Hoist System

Requirements

- An automated hoist system is required to lift the 114kg (250 lb) bell jar cover from the base well and be able to clear a height of 30 inches.
- The hoist system must not be taller than the ceiling height of 13 feet.
- The hoist must be automated and capable of vertical motion with minimal vibrations.
- The system must be safe and easy to operate.

Approach

In order to design the hoist system, an initial investigation is conducted for available free-standing and attached hoist systems. Commercial options as well as a hoist system designed and manufactured at WPI are to be considered. Once a hoist system is chosen, it needs to be integrated with the support structure shown in Figure 1.

2. Integration of the Automated Hoist System with the Support Structure

Requirements

- A support base plate that can hold a 68kg (150lb) hoist. The position of the hoist on the structure table must be investigated in order to accommodate the diffusion pump and the gate valve underneath.
- Support brackets are to be designed in order to attach the hoist to the bell jar.
- The structure should be capable of leveling on an uneven floor. Also, the additional designed parts should not prevent the mobility of the structure.
- The table and the designed parts should have a safety factor of 2 in terms of yield stress and it should not deflect much more than 0.001m (0.0394).

Approach

The support structure and additional designed components (hoist, base well, bell jar, base plate, support bracket, vacuum pump and gate valve) are designed using the solid modeling software Pro/ENGINEER (Pro/E). The structural capabilities under the required loads are analyzed using ProMechanica. Several iterations under various design configurations are explored until a satisfactory configuration is reached.

3. Microflow Analysis and SVF Throughput Evaluation

The microflow analysis in this project will establish a range of mass flow rates that are obtainable within various pressures and orifice diameters. These mass flow rates will then be compared to the operating range of the pump to determine the appropriate conditions in which to carry out experiments.

Requirements

- Nitrogen gas will be the operating fluid.
- Orifice diameter between 0.1 to 100 microns.
- Pressure range between $1.5 \times 10^{-3} – 5.0 \times 10^{-9}$ Torr to match pump operational range.

Approach

To determine the mass flow rate through an orifice, calculations are performed for the range of pressures and orifice diameters. The theory implemented on MATLAB and Excel will be used to carry out this task as well as displaying the results in graphical form. These results will be coupled the throughput analysis of the SVF's pumping system.

2 – Mechanical Design

The previous structure design (Del Vecchio and Loomis, 2009) is the starting point of this project. The table structure was manufactured and the hoist system was installed, allowing full mobility of the table. This met all the design requirements; however, certain aspects of the hoist system made it insecure. Due to safety concerns, the hoist system needed to be altered.

2.1 – Hoist Design

Numerous hoist systems used to operate the facility were investigated and three options were considered:

1. A fully commercial hoist system.
2. A hoist system designed and manufactured at WPI.
3. A hoist with a combination of commercially available parts and parts designed at WPI.

The three options were compared based on the following criteria,

a) Manufacturability
b) Ease of operation
c) Cost of equipment
d) Time

The option to design and manufacture a hoist system at WPI was eliminated first. The design of such a system would require too much time to iterate and manufacture. In addition, the fully designed system will cost approximately as much as a new fully commercial hoist system. The design may also need special attention in the future in case of failure of a part, whereas a commercial system might have parts and technicians more readily available.

A fully commercial hoist system and one that also includes parts designed at WPI were both possible options since they satisfied the criteria. Cost was the greatest concern and the decision was made based on the lower overall cost. All the fully commercial systems had parts that needed to be manufactured in order to attach the hoist system to the bell jar. Therefore, purchasing a commercially available hoist and designing the parts required for the attachment became the focus. The additional parts were manufactured at a local company.

2.1.1 – Research on Available Products

The research included investigating ideas that had already been used on similar vacuum facilities. As referenced in Del Vecchio and Loomis (2009), the automated hoist system from Lesker Company in Figure 9 was deemed to be very costly. The total cost was about $7100.00 without installation or extra mounts.

Figure 9: Kurt J. Lesker Company Hoist System

The hoist system in Figure 10 has a pneumatic lift operated by a pressure pump that raises the shaft to the required height. It is attached to the bell jar at the top by a hook that would normally give the bell jar a lot of freedom in movement. In order to restrict movement of the bell jar, for safety, there are two rails (one of them shown in Figure 10) attached to the bell jar with bearings to hold the bell jar aligned above the base well.

Figure 10: WPI Vacuum Facility Hoist System

KeyHigh & Co. offered another hoist system; the hoist offers a reliable, smooth and quiet operation. Capable of rotating 360 degrees, the complete unit includes a three-switch position and 0.0762m (30 inches) of travel. However, this unit cost $4,195.00 in addition to extra mounting parts that would be added expenses.

Figure 11: Key High Hoist System

2.1.2 – Hoist Purchased

Figure 12: Key High Hoist Purchased

After performing extensive research, a used Key High hoist shown in Figure 12 was found to be the best possible solution for integration into the support structure. The used hoist was offered by E. McGrath Inc., a company that specializes in reconditioned hi-tech equipment. This hoist was chosen because of the better qualifications, but also because of the very low price ($1750.00) compared to similar systems. Another feature of this hoist is the already installed control system, which includes a control panel for lifting, lowering and turning off the hoist.

2.2 Design Iterations

Several iterations were performed to find the best position for the hoist. The hoist needed to be situated in such a way that would provide easy access the rest of the equipment. Another design parameter is the bracket attachment that attaches the hoist to the bell jar. The bracket attachment consists of two side brackets and a U-bracket. The side brackets are welded onto the bell jar for increased structural support and to avoid any leaks from the chamber. The U-bracket serves as attachment hardware that connects the side brackets to the existing holes on the hoist. Lastly, precise measurements were taken in order to construct a CAD model of the hoist. Figure 13 shows the final iteration of the hoist, bracket attachment and bell jar assembled on the support structure.

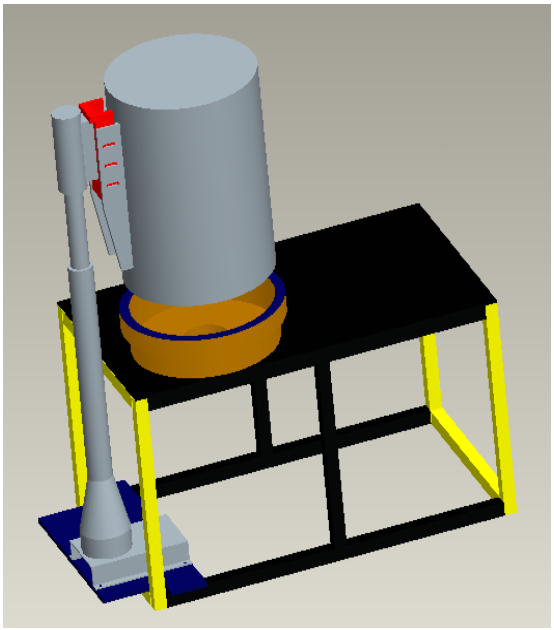

Figure 13: Hoist System on the Structure Table

2.2.1 – Hoist Position

Three different iterations were developed during the design process before a final position for the hoist was chosen. This was mainly due to space constrictions because the hoist had to be placed around other essential equipment. Distance from the bell jar and the height at which the hoist will be attached to the bell jar were other concerns that had to be taken into account.

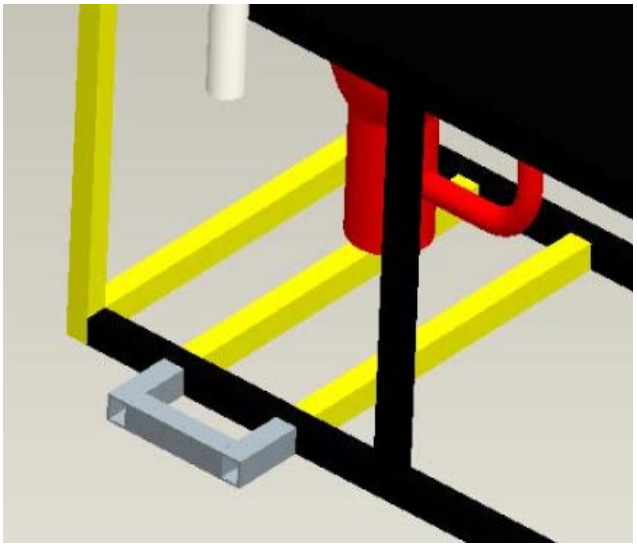

Figure 14: First Iteration of Hoist Base

The first iteration shown in Figure 14 was a design consisting of additional attachments on the underside of the structure. To help support the hoist, two square metal bars would have been welded parallel to each other (yellow bars). Another attachment (grey elbow) would also be welded on the outside of the structure to help position the hoist. The hoist base would be centered on the existing black bar of the support structure. This design was rejected on the basis that the two yellow bars that run the width of the table would interfere with the vacuum system. The diffusion pump would be situated right above the two bars, which would obstruct the position and operation of the pump.

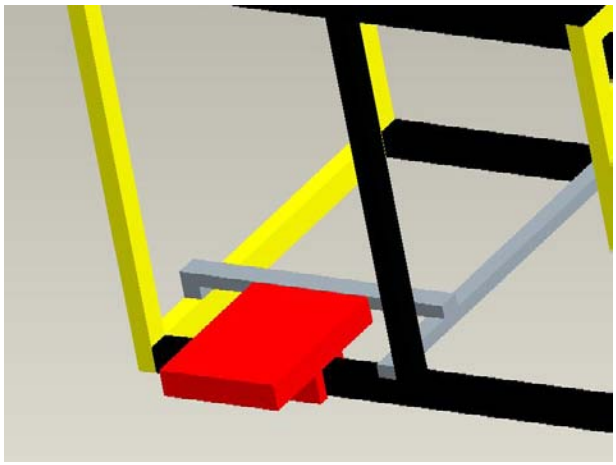

Figure 15: Second Iteration of Hoist Base

The second iteration shown in Figure 15 was a rearrangement of the first iteration. A base plate was designed (red plate) for the hoist to be positioned on. It is attached to the structure with two bars that would be bolted on the structure in order to support the hoist weight. The configuration of the bars is such that they do not interfere with the diffusion pump and would allow easy access. This was an acceptable design, but the gate valve purchased had different dimensions than the gate valve that was previously considered. This created the need for a new design iteration.

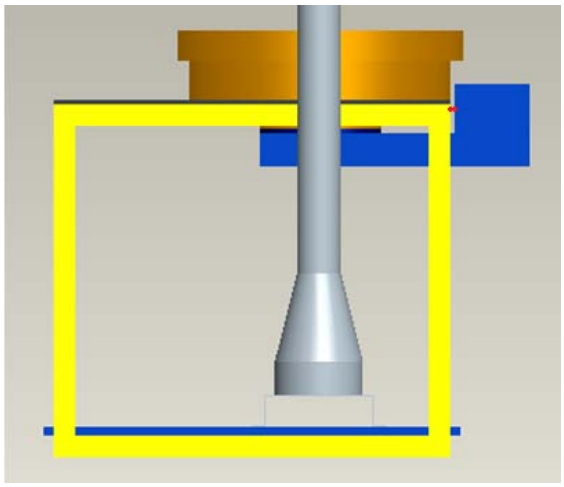

Figure 16: Gate Valve

The gate valve shown in Figure 16 must be placed between the base well and the diffusion pump. Unfortunately, the shape of the gate valve does not allow for easy positioning. The only two choices available were to either cut the existing support structure or move the base well. The configuration chosen was to reposition the base well, gate valve and hoist closer to one side of the structure. Moving the base well meant that changes to the hoist position had to be examined since the bell jar's position was also altered. These changes led to the third and final iteration of the hoist system.

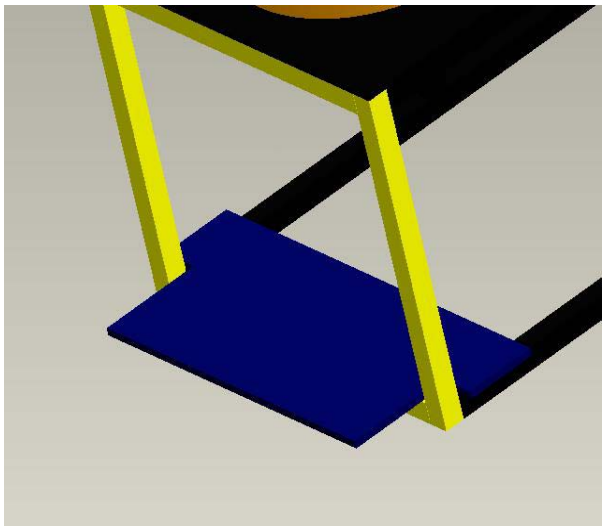

Figure 17: Third Iteration of Hoist Base

In the final iteration, the base plate shown in Figure 17 will be welded to the bottom bars of the support structure. The base plate is made of 0.0177m (.7 inch) thick steel in order to be able to withstand

the weight of the hoist and any fluctuations of forces when the bell jar is lifted or lowered. The hoist was moved to the right side of the table and base plate in order to align it with the new bell jar and base well location.

2.3 – Attachment Bracket

The hoist as purchased could not be connected to the bell jar without some modifications. For this reason a support bracket was designed in order to attach the bell jar to the hoist. After multiple iterations the final design is shown in Figure 18.

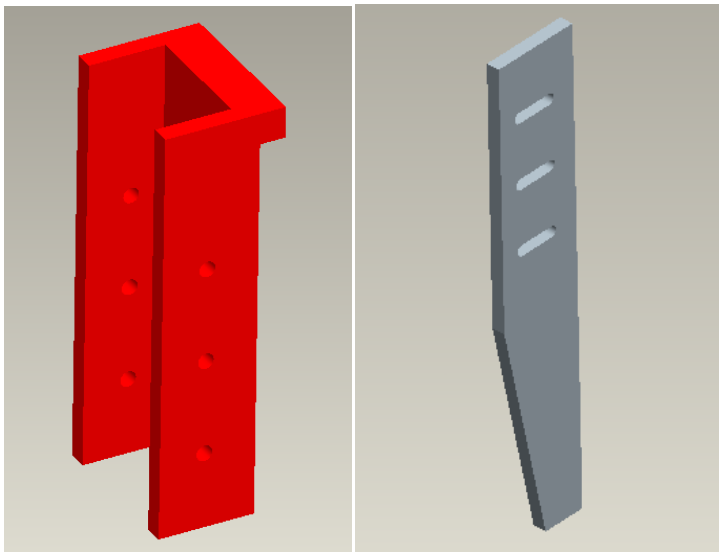

Figure 18: U-Bracket and Side Bracket

The bracket attachment is made of two parts, the first part is a U-bracket (red bracket) and the second is the side bracket (grey bracket). The backside of the U-bracket will be bolted to the top part of the hoist by 6 bolts. The side bracket consists of two pieces that will be welded to the bell jar. The three oval slots on each side bracket were designed to offer a horizontal degree of freedom in order to install the bell jar at the preferred position. A bolt will be used on each slot to secure the side bracket to the U-bracket.

2.4 – Structural Analysis

After design of the structure was completed, stress and deformation analysis was performed for two major reasons. First, the support structure needed to be able to withstand the various added components and their associated stresses. Secondly, various components were added to the structure and minimal deformation needed to be maintained.

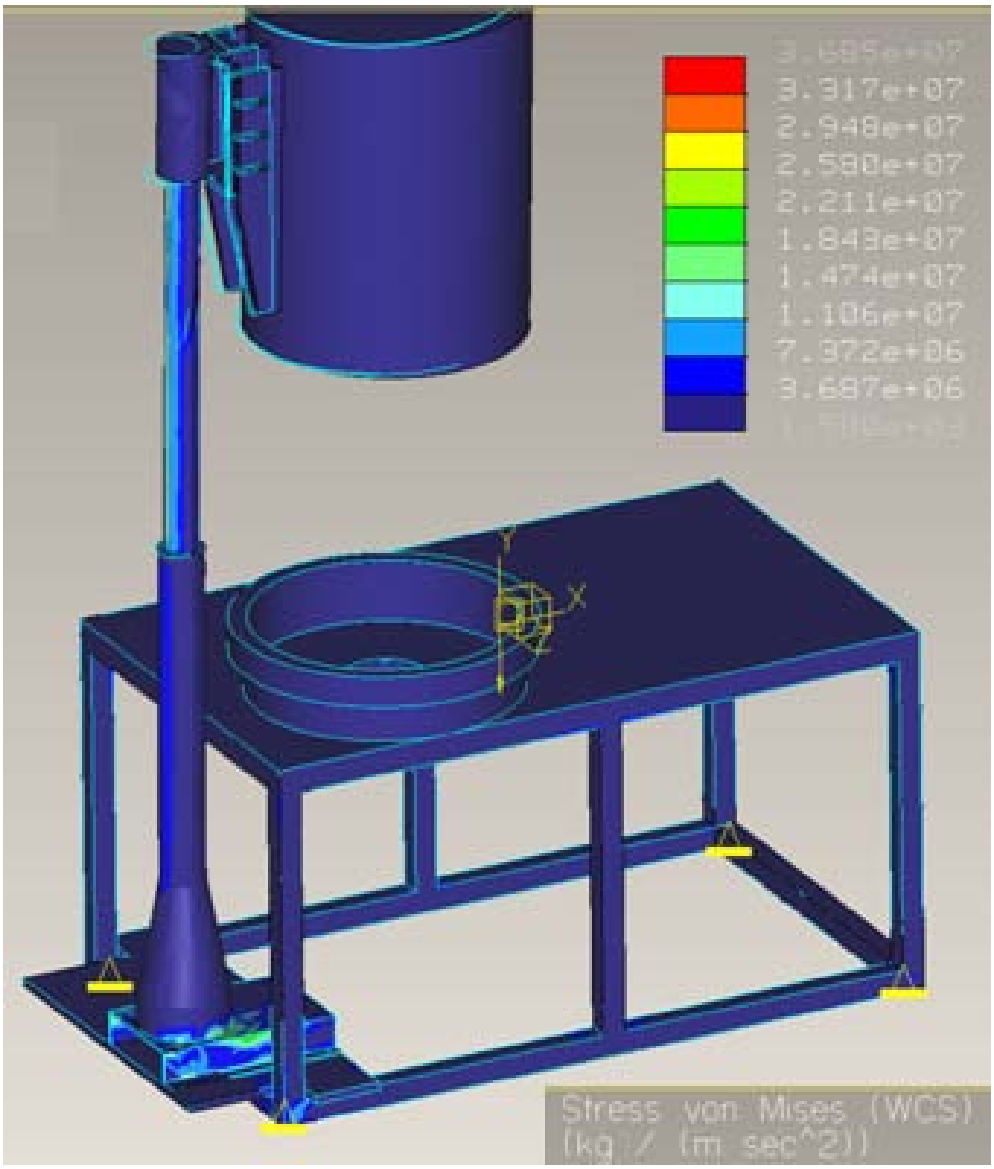

Figure 19: Stresses on the Whole Structure

Mechanica, an extension of Pro/ENGINEER, is used for structural analysis in order to obtain stress and deformation data on the whole structure. All components are made out of structural steel that

has an ultimate strength of 400MPa (58,015.1 psi). The Von Mises stresses, as shown in Figure 19, represent a summary of the results with a maximum value of 24MPa (3,480.9 psi). Another criterion was the deformation on the top surface of the table. Figure 20 shows the deformation results with a 0.0001m (0.00394 in) deflection on the top surface of the table.

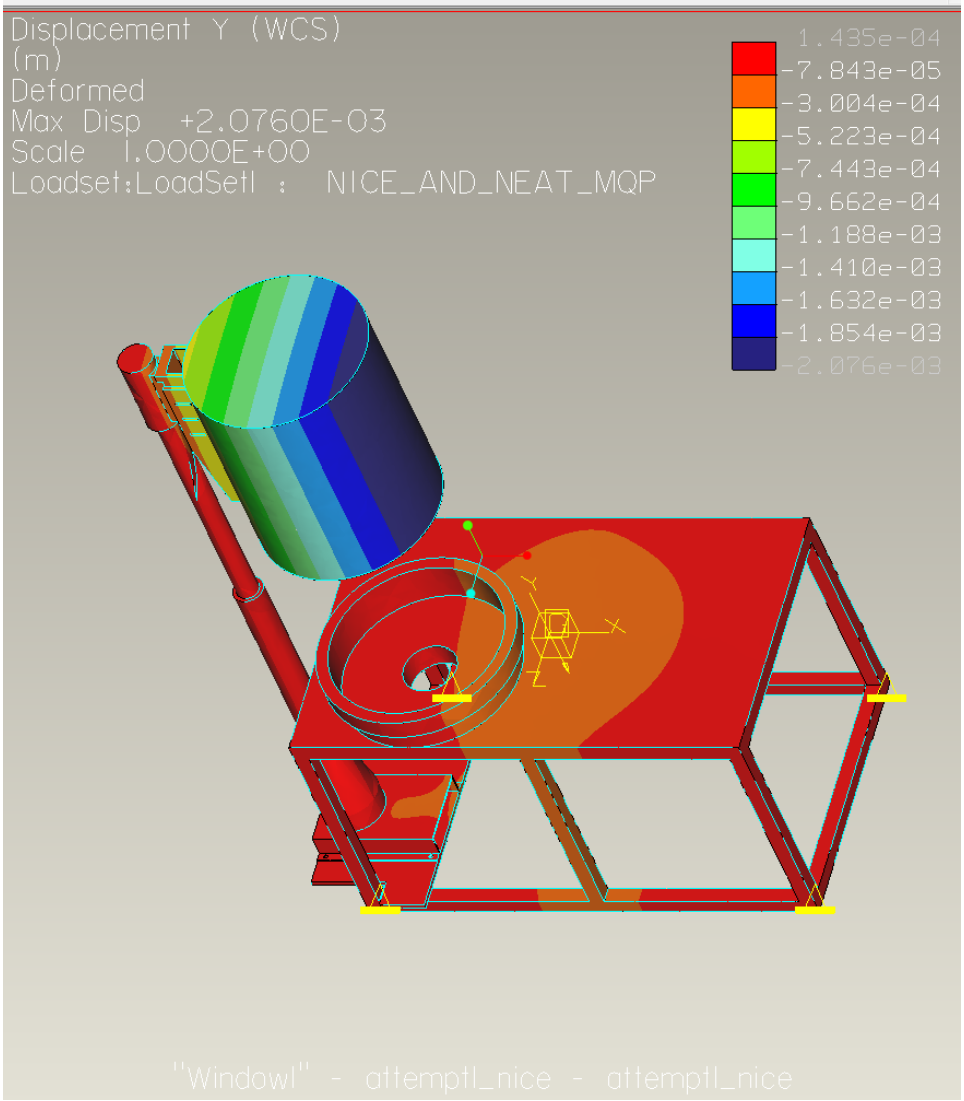

Figure 20: Deformation on the Whole Structure

Deflection analysis was performed with the hoist starting at the maximum position to ensure minimal deformation during operation. The deformations were recorded around the base well surface as the bell jar traveled down to contact position. Table 1 shows the results obtained that confirm small deformations.

Table 1: Deformation Based on Bell Jar Height

Height from Base Well	Deformation in the Y-Direction	Magnitude of Deformation
0.31935 m (12.5799 in)	0.001125 m (0.0443 in)	0.001293 m (0.0509 in)
0.219365 m (8.6364 in)	0.001289 m (0.0507 in)	0.0013286 m (0.0523 in)
0.076565 m (3.0144 in)	0.001183 m (0.0466 in)	0.001226 m (0.0482 in)
0.004365 m (0.1719 in)	0.001166 m (0.0461 in)	0.001162 m (0.0458 in)
0.003365 m (0.1325 in)	0.001123 m (0.0442 in)	0.0011468 m (0.0451 in)

The rigidity of the additional components that were designed also had to be examined. This included analysis on the bracket attaching the hoist to the bell jar and the base plate holding the hoist system. The components were transferred from Pro/E into ANSYS for structural analysis.

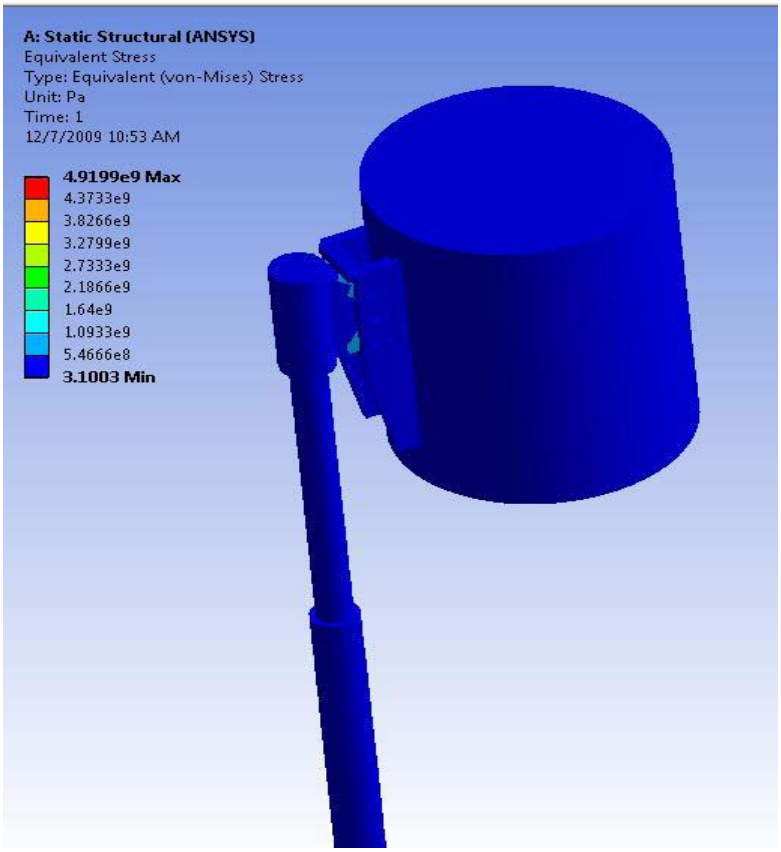

Figure 21: Von Mises Stresses and Deformation of the Support Bracket

With the bell jar attached, representative loads were applied to the support bracket to obtain Von Mises stresses and magnitude of deformation. As shown in Figure 21, a maximum stress of 546MPa (79,190.6 psi) was found. This was a concentrated stress at the back of the bracket, which gives a safety

factor of approximately 2. Also, the magnitude of deformation was less than 1mm, which met the design criterion.

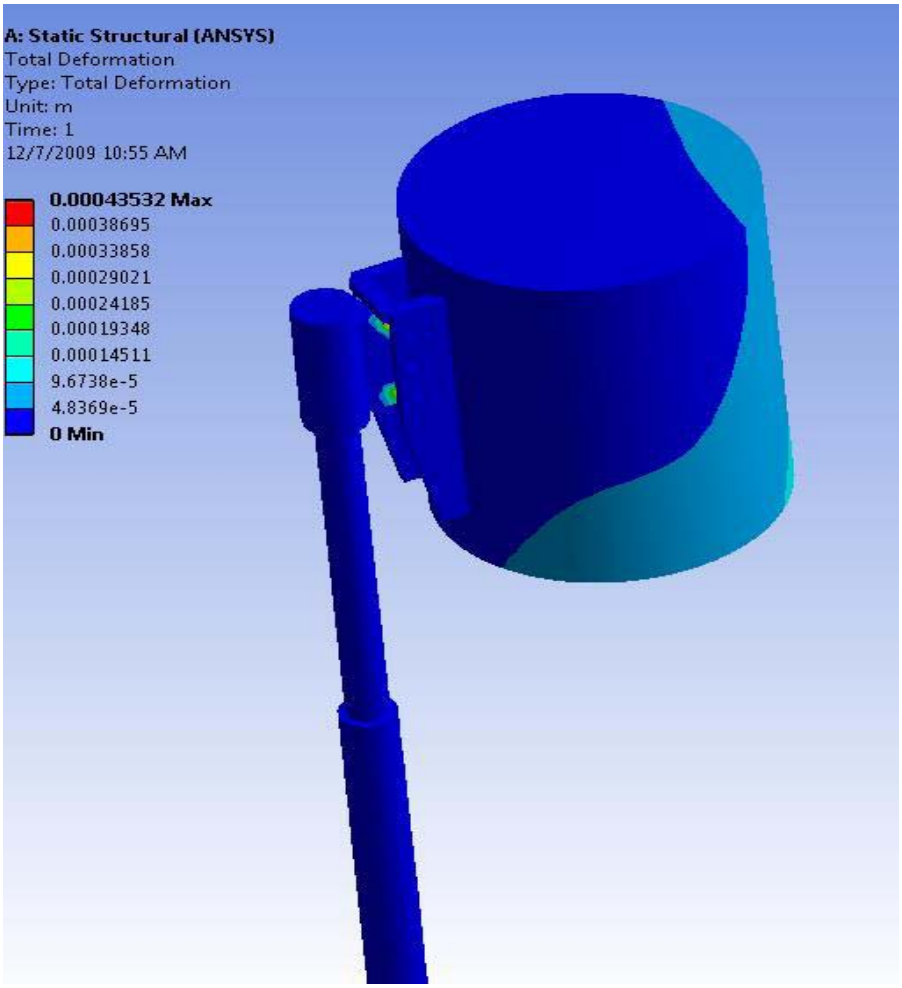

Figure 22: Deformation of the Support Bracket

Furthermore, several tests were performed on the screws attaching the bell jar to the hoist and the hoist to the base plate. The main concern was the tension and compression these screws would undergo. Deformations were found to be less than 0.0005m (0.01969 in) for the screws on the bracket and less than 0.0007m for the screws on the base plate as shown in Figure 24 and Figure 26 respectively. The Von Mises stresses are shown in Figure 23 and Figure 25. They provided a safety factor of 2.2 and assured the rigidity of the structure.

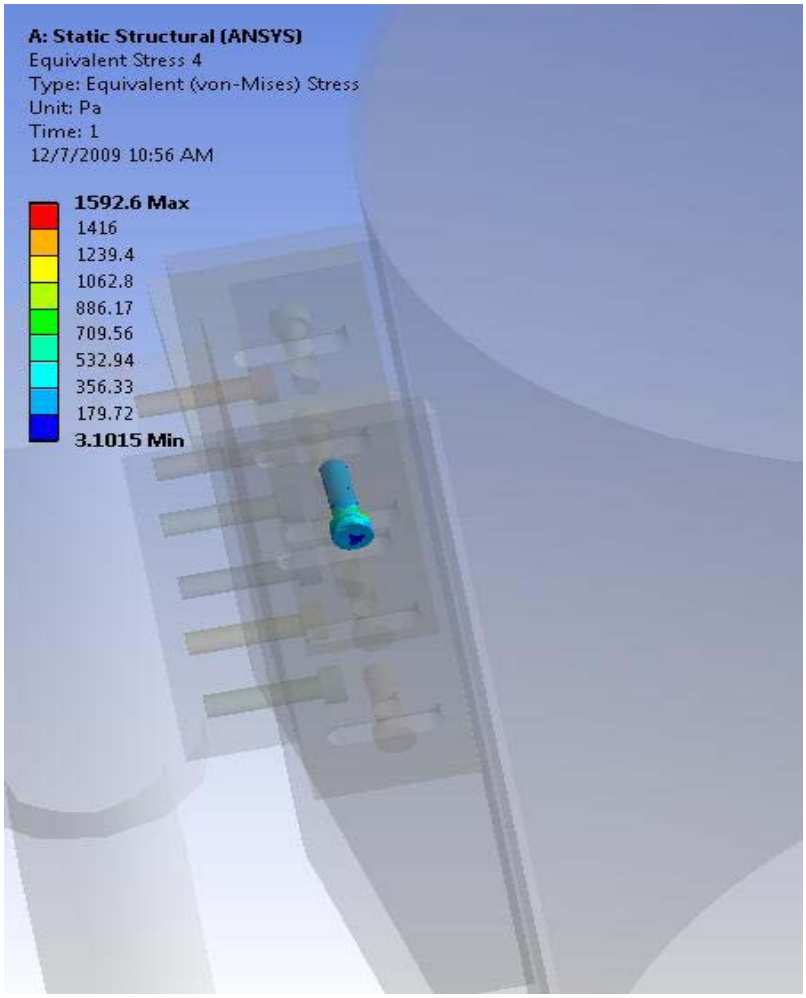

Figure 23: Von Mises Stresses one of the Support Bracket Screw

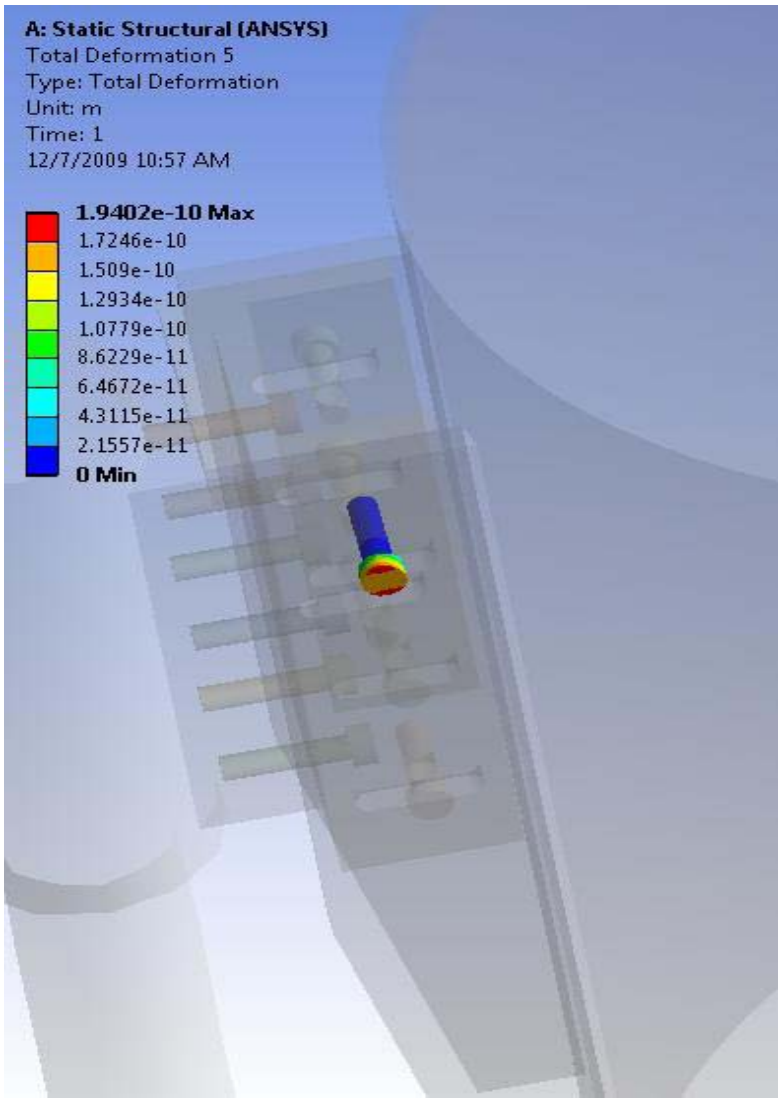

Figure 24: Deformation on one of the support bracket screw

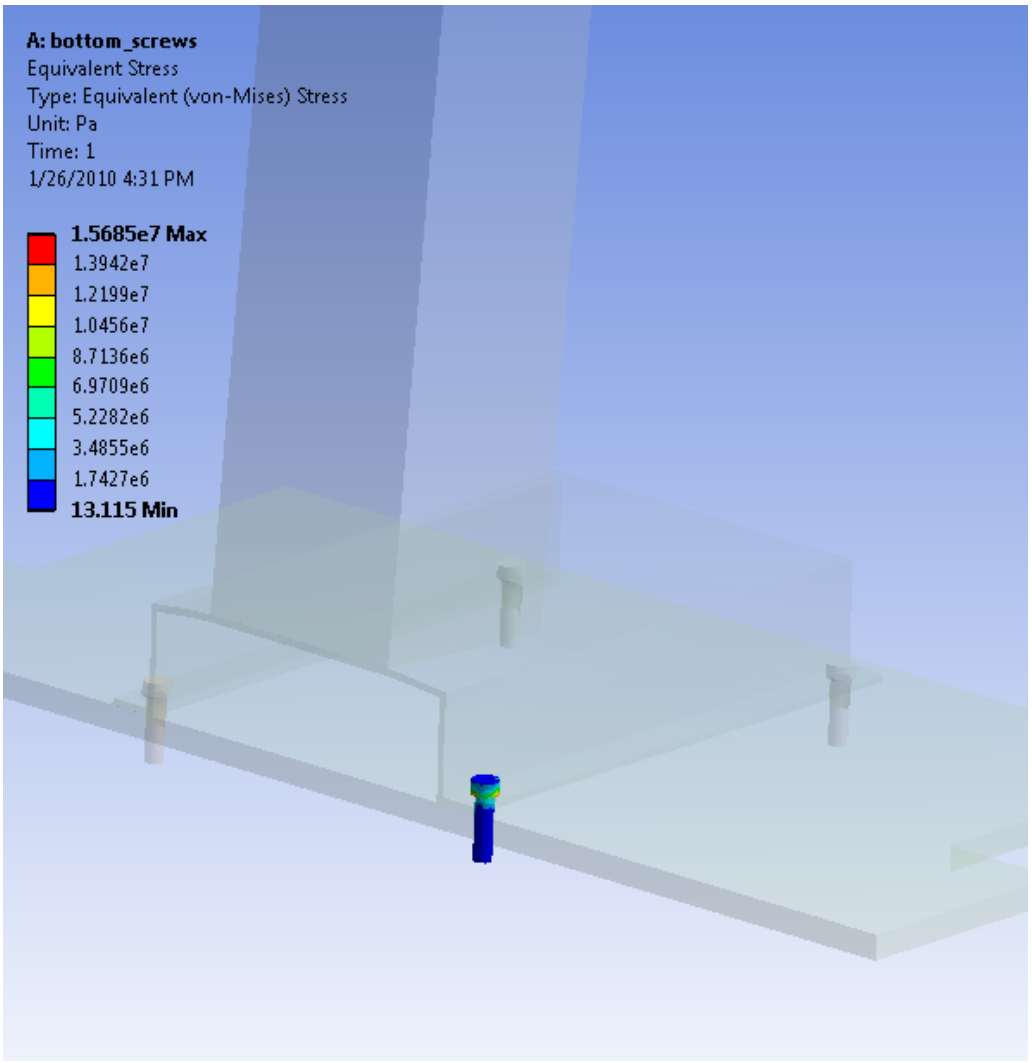

Figure 25: Von Mises Stresses on One of the Bottom Screws

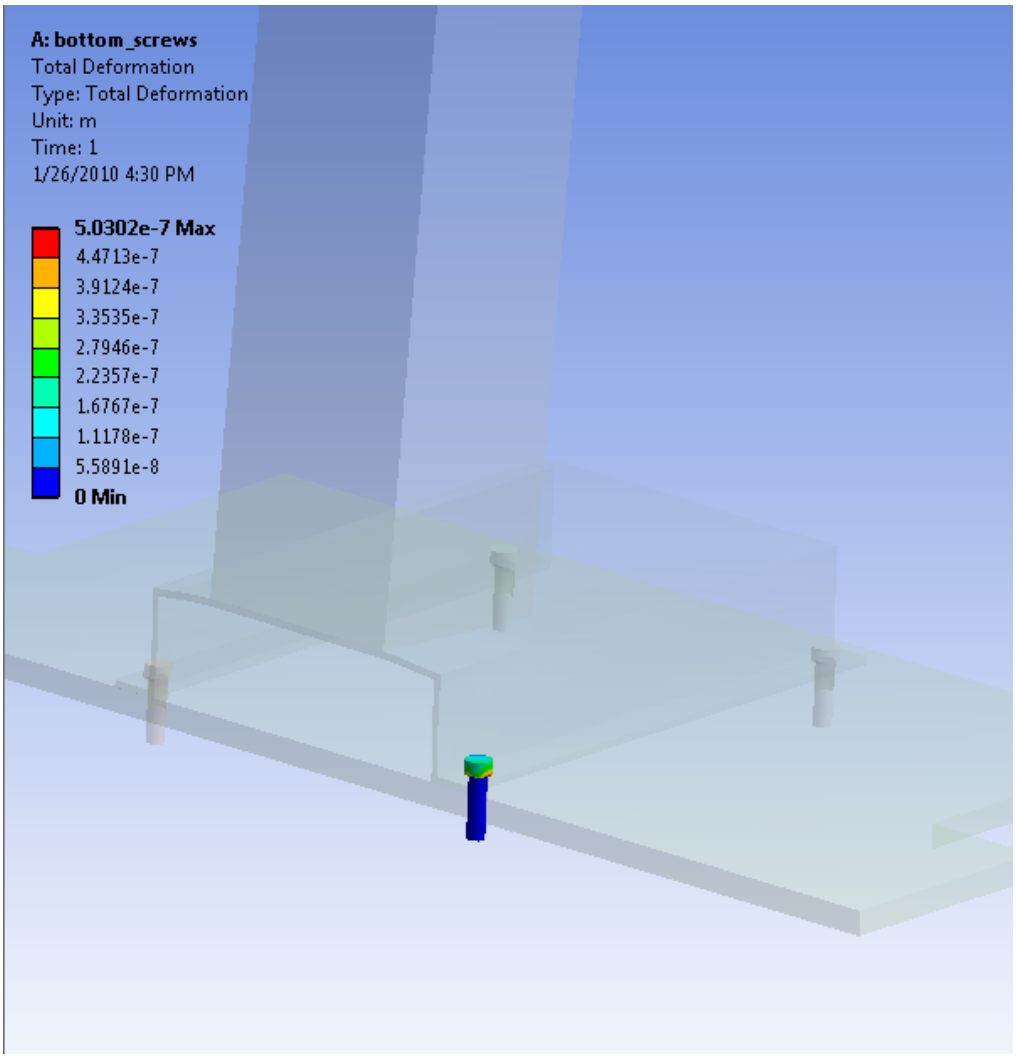

Figure 26: Total Deformation on one of the Bottom Screws

3 – Microflow Analysis

During the creation of the design iterations, fluid analysis and research was performed in order to support the future operation of the Small Vacuum Facility (SVF). The research needed to analyze how gas flow would behave during operation and the limiting factors associated with the flow delivery system and specialized pumps. Once these limiting factors were determined, it was then possible to calculate a range of mass flow rates that can be achieved in the facility.

3.1 – Pumping Operations

The operation of the Small Vacuum Facility in Higgins Laboratories 314 is dependent on the ability of the equipment to control pressure variations in the reservoir and in the test chamber. The facility's pressure conditions are controlled through various apparatus. Significant among these are the pumps, which are responsible for removing gases from the chamber to maintain pressure conditions. The purpose of this project is to investigate the expansion of nitrogen from a microjet into a vacuum. It is therefore necessary to investigate whether the pumps can drain out the gas faster than the reservoir is adding it to the chamber. To do this it is essential to understand basic pumping theory and to calculate the maximum pumping speeds at which the pumps can operate under different testing conditions. In addition it is necessary to carry out a microfluid analysis in order to investigate the rate of mass flow that can be discharged by a flow delivery system through either a microscopic orifice or tube. This chapter will provide background about SVF operations that include general pumping concepts and mass flow computations both in delivery systems and diffusion pumps.

3.1.1 – Diffusion Pump Background

In order to create a vacuum in the chamber, gas will be removed from the interior using a combination of two pumps. The pumps used in the facility are a Varian VHS-6 Diffusion Pump and a Varian DS602 3Ph Dual Stage Rotary Vane (Mechanical) Pump. The setup of the complete system can be seen in Figure 27.

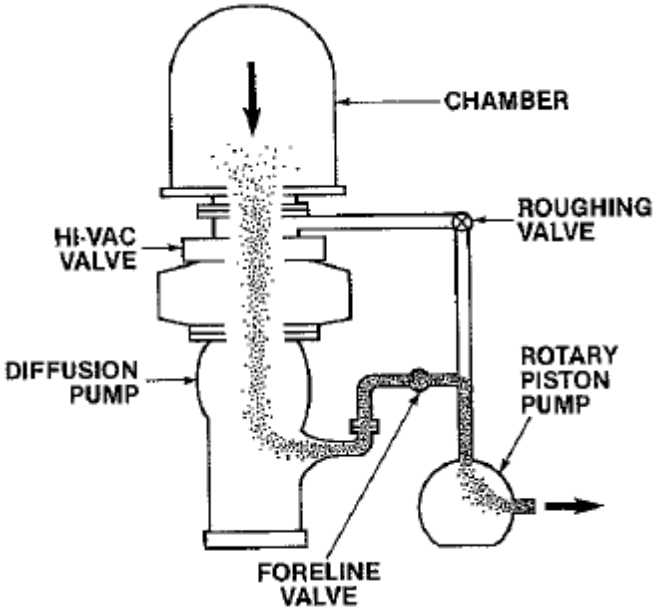

Figure 27: Schematic of Vacuum System (Varian, 1992)

A diffusion pump works by heating the pump fluid in the oil reservoir. Once the fluid is heated, the vapors travel upward and are accelerated out through several stages of nozzles as jets. The fluid is directed towards the outer walls that are typically cooled with water. When the fluid vapors reach the cool walls they are condensed back into a liquid and drained to the reservoir where they are reheated. The pump compresses gas from the chamber in the jet stream and pushes it out the exhaust. This creates a vacuum or what is generally known as a pumping operation. The gases are then pumped through a mechanical pump before being expelled into the atmosphere. A general schematic of the parts of a diffusion pump is shown in Figure 28.

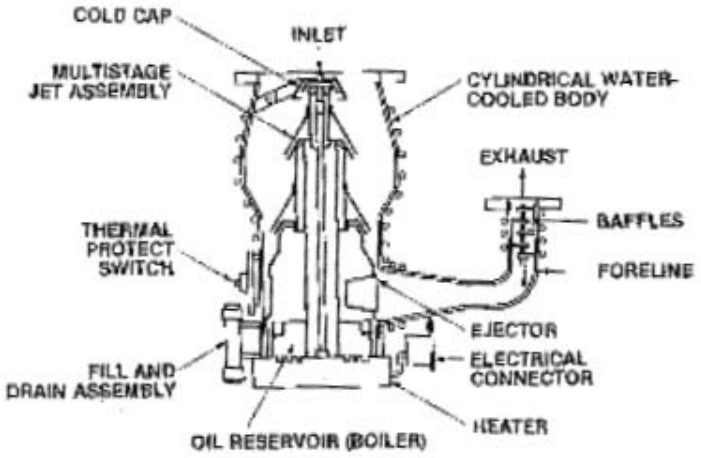

Figure 28: Diffusion Pump Schematic (Varian, 1992)

The diffusion pump cannot pump directly to atmospheric conditions because the pressure in the foreline must be below the pressure in the boiler. If this is not maintained then pumping is not possible due to backstreaming. In order to guarantee the system will function properly, the mechanical pump must be capable of handling the gas output of the diffusion pump. As long as this is ensured, mechanical failure will be the most likely be the cause of exceeding the forepressure. To prevent backstreaming, a baffle is used between the diffusion pump and the mechanical pump. A schematic of the mechanical pump is shown in Figure 29.

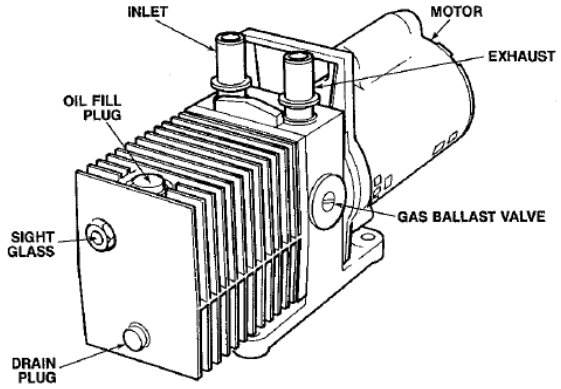

Figure 29: Mechanical Pump (Varian, 1992)

Another important factor to consider about the pump is the maximum inlet pressure. The inlet pressure must be lower than the pressure where the top jet fails. If the inlet pressure is above that then the pump will not function. The mechanical pump is used to lower the inlet pressure. Exceeding the critical inlet pressure can be caused by operational errors, heater failure or large leaks (Varian, 1992). Technical data for the mechanical pump can be found in Table 2.

Table 2: DS602 Mechanical Pump Specifications (Varian, 1992)

TECHNICAL DATA	Hz	UNITS	DS102	DS202	DS302	DS402	DS602
FREE AIR DISPLACEMENT	60	l/min (cfm)	114 (4)	192 (6,8)	285 (10)	410 (14,5)	605 (21,4)
	50	l/min (m^3/h)	95 (5,7)	160 (9,6)	237 (14,2)	342 (20,5)	540 (30,2)
PUMPING SPEED *	60	cfm	3,5	5,8	8,2	12,3	18,3
	50	m^3/h	5	8,3	11,6	17,4	26
ULTIMATE PARTIAL PRESSURE *		mbar	10^{-4}	10^{-4}	10^{-4}	10^{-4}	10^{-4}
ULTIMATE TOTAL PRESSURE *		mbar	$2 \cdot 10^{-3}$	$2 \cdot 10^{-3}$	$2 \cdot 10^{-3}$	$2 \cdot 10^{-3}$	$2 \cdot 10^{-3}$
ULTIMATE TOTAL PRESSURE WITH GAS BALLAST *		mbar	$2 \cdot 10^{-2}$	$2 \cdot 10^{-2}$	$2 \cdot 10^{-2}$	$1 \cdot 10^{-2}$	$1 \cdot 10^{-2}$
WATER VAPOR TOLERANCE		mbar	15	15	20	30	30
WATER VAPOR CAPACITY		g/h	60	100	160	350	550
OIL CAPACITY min/max		l	0,3/0,5	0,4/0,6	0,4/0,6	0,6/1	0,6/1
MOTOR RATING 1ph	50/60	kW	0,45/0,55	0,45/0,55	0,45/0,55	0,75/0,90	0,75/0,90
MOTOR RATING 3ph	50/60	kW				0,75/0,90	0,75/0,90
NOMINAL ROTATION SPEED	50	rpm	1500	1500	1500	1500	1500
	60	rpm	1800	1800	1800	1800	1800
OIL TEMPERATURE		°C	50	50	52	70	72
(pump operating) **		°F	122	122	126	158	162
Installation category	II						
Pollution degree	2						
OPERATING TEMPERATURE RANGE		°C	12 - 40	12 - 40	12 - 40	12 - 40	12 - 40
WEIGHT		Kg	22	24	24	36	36
		lb	48	53	53	79	79
INLET FLANGE		DN	25KF	25KF	25KF	25KF	25KF
EXHAUST FLANGE		DN	25KF	25KF	25KF	25KF	25KF
Dimensions (cf. also next table):							
- length, 1ph		mm	454	491	491	530	530
- width		mm	134	134	134	164	164
- height		mm	212	212	212	242	242
Input single phase versions ***							
Nominal voltages:	50	V	100 200-240	100 200-240	100 200-240	100 200-240	100 200-240
	60	V	100-120 200-230	100-120 200-230	100-120 200-230	100-120 200-230	100-120 200-230
Maximum currents:	50	A	8,8 5,4	8,8 5,4	8,8 5,4	11,8 6,2	11,8 6,2
	60	A	8,8 4,4	8,8 4,4	8,8 4,4	12,8 6,4	1,8 6,4

3.1.2 – Basic Pump Theory

In basic pump theory, three different types of pumps are defined across a range of operating pressures: mechanical pumps, high vacuum pumps, and ultrahigh vacuum pumps (diffusion). Because this project is focused on testing microjets well below atmospheric conditions, a high vacuum pump with an operating range of 1.5 X 10^{-3} – 5.0 X 10^{-9} Torr will be incorporated. At these very low pressures, gases exhibit free molecular flow properties, which means that molecular movement is unpredictable. Thus, the diffusion pump needs to have a wide opening or good conductance path in order to accommodate the free molecular flow. Conductance is the amount of gas that passes through an opening in a given amount of time. It is measured in units of $\left[\frac{l}{s}\right]$ (Varian, 1992). Another term for conductance is also known as air speed, which is expressed in the same units and used widely in pumping calculations.

Conductance and air speed are terms that define the performance of how fast a vacuum pump can expel gases. The measurement of this performance is termed pumping speed, *S*, which is in units of $\left[\frac{l}{s}\right]$, or $\left[\frac{ft^3}{min}\right]$, where $\forall$ is the volume of the gas, given by:

$$S = \forall / t \tag{3.1}$$

Pumping speed expresses how fast the vacuum can pump a gas, but it does not tell how much work the pump is performing. In order to measure the work performed by the pump, the number of molecules of gas being removed from the vacuum chamber per unit time needs to be considered. The amount of molecules in a vacuum chamber is measured by multiplying the pressure [*Torr*] by the volume [*l*] of the chamber. This expression is a measure of work known as gas load. In order to measure the power or capacity of the pump, the amount of worked performed by the pump per unit time is used. This term is defined as throughput and is typically expressed in units of $\left[\frac{Torr\ -1}{s}\right]$ given by:

$$Q = PS \tag{3.2}$$

Throughput is work per unit time, a measurement of power. It is the product of the pumping speed of the diffusion pump and the pressure inside the vacuum chamber. Therefore, both pumping speed and chamber pressure must be defined. These parameters are crucial at different testing conditions in order to calculate how many molecules the pump is capable of pumping out per unit time. This theory will be used, along with the specifications of the pumps in order to calculate the capacity of the pumps at

different testing pressures. With this information, the maximum mass flow that can be pumped out of the vacuum chamber by the pumps can be calculated once the flow delivery system limits are determined.

3.2 – Flow Through an Orifice

To determine the limits of the flow delivery system, a detailed fluid analysis must be performed. Flows through orifices are characterized into three different regimes: continuum, transitional and rarefied. To classify which regime a particular flow falls into, the Knudsen number is used. The Knudsen number is a dimensionless quantity defined by the ratio of the mean-free path, λ, of the molecules to a characteristic length, in this case the diameter, *D* [m], of the orifice.

$$Kn = \frac{\lambda}{D} \tag{3.3}$$

The mean-free path of the molecules is dependent on the molecular diameter, *d* [m], and the number density, *n* [m^{-3}], of the gas.

$$\lambda = \frac{1}{\sqrt{2}\pi d^2 n} \tag{3.4}$$

The number density is used in the derivations of particle flux when implementing Boltzmann's equations. It relates pressure, *p* [Pa], temperature, *T* [K], and the Boltzmann's constant, *k*, where with the ideal gas law:

$$n = \frac{p}{kT} \tag{3.5}$$

and:

$$k = 1.38\text{E-}23 \left[\frac{m^2 kg}{s^2 K}\right]$$

Each of the different regimes corresponds to a particular range of Knudsen numbers. The equations that are used to predict the behavior of the flow through an orifice change based on what regime the flow falls into. If the diameter of the orifice is much larger than the mean-free path of the molecules,

then the Knudsen number will be very small and the flow would be in the continuum regime ($0.01 \geq Kn > 0$). For flows through orifices in which case the diameter is substantially smaller than the mean-free path, the flow is characterized by the rarefied regime ($Kn \geq 10$). Any flow with a Knudsen number in between 0.01 and 10 is in the transitional regime. The behaviors of these flows are difficult to define by any one fluid dynamic theory. Therefore, the assumption is made in this analysis that any flow with a Knudsen number between 1 and 10 will also be included in the rarefied regime and any flows with a Knudsen number less than 1 will be in the continuum regime.

3.2.1 – Continuum Regime

For gas flows that fall into the continuum regime, the hydrodynamic escape formula of the molecular effusion theory can be used to predict the conditions at the exit of the orifice (Gombosi, 1994). In its most general interpretation, the hydrodynamic escape theory considers the very simple model of two reservoirs connected by a relatively large orifice in comparison to λ. A schematic is shown in Figure 30.

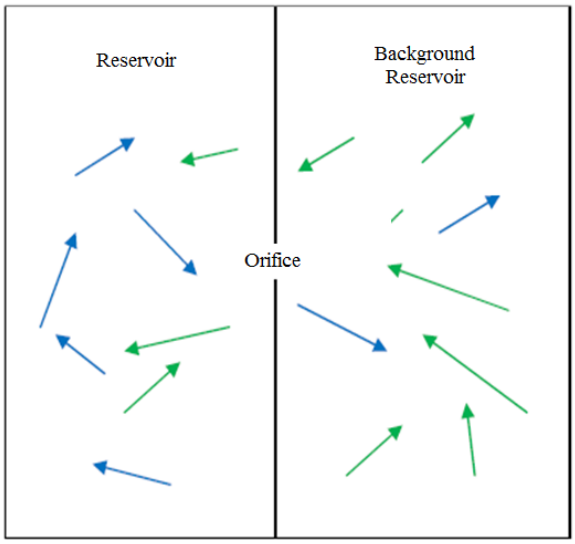

Figure 30: Reservoir Approximation for Orifice Theory

In Figure 30, test conditions in the reservoir are denoted by variables with a subscript *r* such as pressure and number density denoted by p_r and n_r, respectively. The background reservoir of the facility represents the test chamber where conditions are denoted by a subscript *b* where p_b and n_b are the pressure and number density. It is assumed in this theory that $p_r \geq p_b$. Conditions at the orifice are represented by the variables *p* for pressure, *n* for number density and *u* for flow velocity without subscripts.

The flow is approximated by a steady state adiabatic outflow with no external work. In other words, total internal energy is constant and therefore Bernoulli's equation can be used to obtain an expression in terms of flow velocity, $u\left[\frac{\mathrm{m}}{\mathrm{s}}\right]$, and number density:

$$\frac{\gamma}{\gamma-1}\frac{p}{mn}+\frac{1}{2}u^2=\frac{\gamma}{\gamma-1}\frac{p_r}{mn_r} \tag{3.6}$$

In equation (3.6), γ is the specific heat ratio and m is the molecular mass. Because the flow is also adiabatic, the following expression for adiabatic flow can be used in terms of pressure and number density (Gombosi, 1994):

$$\frac{p_r}{n_r^{\gamma}}=\frac{p}{n^{\gamma}} \tag{3.7}$$

This can be solved for orifice number density, n:

$$n=n_r\left(\frac{p}{p_r}\right)^{\frac{1}{\gamma}} \tag{3.8}$$

By substituting n_r into equation (3.6), and solving for, u an expression for flow velocity is obtained:

$$u=\sqrt{\frac{2}{\gamma-1}\frac{\gamma p_r}{mn_r}\left[1-\frac{p}{p_r}^{\frac{\gamma-1}{\gamma}}\right]} \tag{3.9}$$

This expression is practical for subsonic flows through orifices in which case the flow velocity is less than the local sound velocity at the orifice. According to the hydrodynamic theory of flows through orifices, the flow is in the continuum regime. It is therefore considered compressible and it is assumed that the flow will choke at the orifice. For this reason, "The flow velocity in the orifice [nozzle throat] cannot be higher than local sound velocity." (Jahns, 2009). The speed of sound, a_r, at the reservoir can be expressed by:

$$a_r=\sqrt{\frac{\gamma p_r}{mn_r}} \tag{3.10}$$

The speed of sound at the orifice is derived using the adiabatic equation (3.7) and the definition of sound speed (3.10).

$$a = \sqrt{a_r^2 \left(\frac{p}{p_r}\right)^{\frac{\gamma-1}{\gamma}}} \tag{3.11}$$

The mass flow rate, $\dot{m}$, for subsonic flow through the orifice is found by substituting the velocity equation (3.9) in the following equation:

$$\dot{m} = \rho u A \tag{3.12}$$

This gives the following equation of mass flow rate for subsonic flow, which will be used in the MATLAB code and Excel program:

$$\dot{m} = \frac{A p_r}{RT} \sqrt{\frac{2}{\gamma - 1} \frac{\gamma p_r}{m n_r} \left[1 - \frac{p}{p_r}^{\frac{\gamma-1}{\gamma}}\right]} \tag{3.13}$$

This equation is not valid when the orifice pressure is equal to the reservoir pressure. If $p/p_r = 1$, then there will not be any mass flow through the orifice. The mass flow rate reaches a maximum when the orifice pressure is equal to a critical pressure, p_c, defined as:

$$p_c = p_r \left(\frac{2}{\gamma + 1}\right)^{\frac{\gamma}{\gamma-1}} \tag{3.14}$$

At this critical pressure, there is also a critical velocity, u_c, also at a maximum.

$$u_c = \sqrt{\frac{2\gamma}{\gamma + 1} \frac{p_r}{m n_r}} \tag{3.15}$$

In the special case in which the background pressure is at a critical pressure due to sonic flow through the orifice, the mass flow rate $\dot{m}$ is calculated in a similar manner using the flow velocity expression obtained for critical velocity (3.15):

$$\dot{m}_c = \rho u_c A \tag{3.16}$$

This gives the following equation for mass flow rate at the critical condition of the continuum regime, which will again be used in the MATLAB code and Excel program:

$$\dot{m}_c = \frac{A p_r}{RT}\sqrt{\frac{2\gamma}{\gamma+1}\frac{p_r}{m n_r}} \tag{3.17}$$

3.2.2 – Rarefied Regime

The next regime to be considered is the rarefied. It is characteristic of flows through orifices in which the diameter is assumed to be substantially smaller than the mean-free path of the molecules, resulting in a high Knudsen number ($kn \geq 10$). At a higher Knudsen number, collisions between molecules are much less frequent; this means that molecules will pass through the orifice without seeing and/or colliding with one another. To predict the behavior of the flow through the orifice in this case, the kinetic effusion theory is used. By examining the velocity distribution function of the molecules escaping through the orifice, it can be found that only the molecules that have a velocity component in the direction perpendicular to the orifice will escape the tank. This is illustrated by the red arrows in Figure 31:

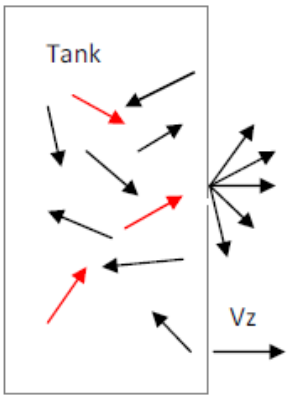

Figure 31: Kinetic Effusion Through an Orifice

Using a truncated Maxwell-Boltzmann distribution function, equation (3.18), the escape flux of the molecules from the reservoir can be calculated (Gombosi, 1994). In Figure 31, the positive 'z' axis is in the direction out of the orifice.

$$F_r = \begin{cases} n_r \left(\frac{m}{2\pi k T_r}\right)^{\frac{3}{2}} e^{-\frac{m}{2kT}(u_x^2+u_y^2+u_z^2)} if u_z > 0 \\ 0 \qquad\qquad\qquad\qquad\qquad\qquad if u_z \leq 0 \end{cases} \tag{3.18}$$

Consider a group of molecules with velocity vectors, *u*, escaping an orifice of area, *dS*, during a time interval, *dt*. Before the molecules escape through the orifice, they are assumed to be contained in an 'impact cylinder' at the beginning of the time interval, *dt*. This impact cylinder has dimensions of a base with the same area as the orifice, *dS*, and a height of $u_z dt$, as illustrated in Figure 32.

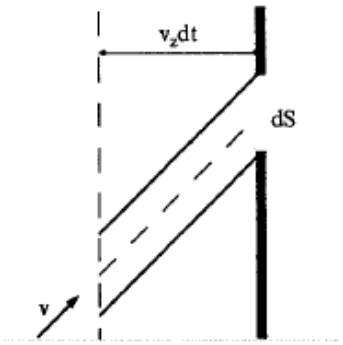

Figure 32: Impact Cylinder Demonstrating the Path of the Escaping Molecules (Gambosi, 1994)

Given these dimensions, the volume of the cylinder is:

$$dV_{impact} = u_z dt dS \tag{3.19}$$

Therefore, the number of molecules with velocities between *u* and $u + d^3u$, that impact the area, *dS* and escape through the orifice in the time interval *dt*, can be calculated using the following expression:

$$d^6N = F_r d^3u dV_{impact} = u_z F_r d^3u dt dS \tag{3.20}$$

According to the kinetic effusion theory, the escape flux is calculated with the help of the distribution function of escaping particles, F_r, and by using expression (3.20) for the number of particles that pass through the orifice.

$$j_r = \int_{-\infty}^{\infty} du_x \int_{-\infty}^{\infty} du_y \int_{-\infty}^{\infty} du_z u_z F_r(\boldsymbol{u}) \tag{3.21}$$

Where u is the particle velocity expressed as a vector. Noticing that particles with $u_z \leq 0$ cannot leave Reservoir 1 through the orifice and carrying out this substitution results in a very simple expression for escape flux $\left[\frac{\#\ \text{particles}}{\text{m}^2\text{s}}\right]$:

$$j_r = n_r \sqrt{\frac{kT_r}{2\pi m}} \tag{3.22}$$

From the distribution function (3.18), a definition for the mean speed of a gas in equilibrium can be obtained, which is denoted by:

$$\bar{u} = \sqrt{\frac{8kT}{\pi m}} \tag{3.23}$$

The escape flux expression (3.21) can therefore be expressed as:

$$j = \frac{1}{4} n \bar{u} \tag{3.24}$$

If the conditions for kinetic theory are satisfied in both reservoirs and the mean free path of the molecules inside the reservoirs are much larger than the diameter of the orifice, then molecular scattering can be assumed from reservoir *r* to the chamber and vice versa. This means that molecules escape from the reservoir, *r*, to the test chamber in the same manner in which molecules in the test chamber escape to the reservoir, *r*; without any molecular collisions. This essentially means that the escape fluxes from both reservoirs do not influence each other and therefore, the net particle flux in the rarefied regime is calculated by taking the differences in fluxes. This is illustrated in Figure 30.

$$j_{net} = j_r - j_b = \frac{1}{4}(n_r \bar{u}_r - n_b \bar{u}_b) \tag{3.25}$$

This equation can be written in terms of pressure given the expression for the number density, *n*, from equation (3.8) and further simplified into:

$$j_{net} = \frac{1}{4}\sqrt{\frac{8}{\pi m k}}\left(\frac{p_r}{\sqrt{T_r}} - \frac{p_b}{\sqrt{T_b}}\right) \tag{3.26}$$

If the temperatures in the reservoir and test chamber are assumed to be equal, $T_r = T_b = T$, this further simplifies the equation to:

$$j_{net} = \frac{p_r - p_b}{\sqrt{2\pi m k T}} \tag{3.27}$$

The mass flow, with units of $\left[\frac{kg}{s}\right]$, through the orifice is then given by the net flux:

$$\dot{m} = m j_{net} A \tag{3.28}$$

or further simplified to:

$$\dot{m}_{net} = A(p_r - p_b)\sqrt{\frac{m}{2\pi k T}} \tag{3.29}$$

3.3 – Tube Flow

Tube flow is also reviewed to develop a better understanding of all of the different regimes and conditions of flow that would exist in the Small vacuum chamber facility, but will not be covered in as much depth as orifice flow. Similar to flows through an orifice, flows through a tube can be characterized into the same different regimes: continuum, transitional and rarefied. The regimes are determined using the same methods detailed in section 3.2.

3.3.1 – Continuum Regime

3.3.1.1- Long Round Tubes

For long round tubes that fall within the continuum regime, the general convention is to use the Hagen-Poiseuille equation, here in terms of throughput (O'Hanlon, 2003):

$$Q = \frac{\pi d^4}{128\eta l}\frac{(P_1 + P_2)}{2}(P_1 - P_2) \tag{3.30}$$

Where η is the viscosity and l is the characteristic length. To convert this to mass flow, one must multiply by the molecular weight, m, and divide by the universal gas constant, R, and the temperature, T.

$$\dot{m} = \frac{Qm}{RT} \tag{3.31}$$

Using this relation, the mass flow rate can be solved for using equation (3.31).

$$\dot{m} = \frac{m\pi d^4}{128\eta lRT}\frac{(P_1 + P_2)}{2}(P_1 - P_2) \tag{3.32}$$

3.3.1.2 – Short Round Tubes

Next is the case of short, round tubes that fall within the continuum regime. These tubes do not obey the Poiseuille equation. The equation that one uses for this type of flow regime depends on whether the flow is choked or not. If the flow is not choked, the orifice flow equations for the continuum regime are used, which are detailed in section 3.2.1. If the flow is choked, equation (3.30) for throughput can be used. Alternatively, equation (3.32) for mass flow can be used where $P_1 = P_x$. P_x is the inlet pressure to the tube and $P_2 = 0$ is the output pressure.

3.3.2 – Rarefied Regime

3.3.2.1 – Long Round Tubes

For long round tubes in the rarefied regime, the diffusion method is used to model the flow. For circular tubes the conductance is found to be (O'Hanlon, 2003):

$$C_{tube} = \frac{\pi}{12} v \frac{d^3}{l} \tag{3.33}$$

where v is the thermal velocity of the gas. To obtain the expression for mass flow rate from conductance, first multiply by the pressure difference, which gives throughput, Q, as shown by equation (3.34).

$$Q = C(P_1 - P_2) \tag{3.34}$$

Mass flow rate can then be found from the throughput, resulting in an expression that is valid for short round tubes with a value approaching the ratio *l/d*.

$$\dot{m} = \frac{m\pi}{12RT} v \frac{d^3}{l} (P_1 - P_2) \tag{3.35}$$

3.3.2.2 – Short Round Tubes

For short tubes with ratios of *l/d* approaching zero, the equation reduces to the orifice theory conductance in the rarefied regime, which can be modified to obtain mass flow rate. The mass flow rate equation for this case is detailed in section 3.2.2. For ratios of *l/d* approaching infinity, the conductance approaches equation (3.34), which can be used to find the mass flow rate, equation (3.35). For cases that do not fall into these extreme conditions, the relation below can be used to obtain conductance.

$$\frac{1}{C_{total}} = \frac{1}{C_{tube}} + \frac{1}{C_{aperture}} \tag{3.36}$$

Once C_{total} is determined, it can then be rearranged using the relation between mass flow and throughput and the relation between conductance and throughput simultaneously.

$$\dot{m} = \frac{mC_{total}}{RT} (P_1 - P_2) \tag{3.37}$$

3.4 – Calculation of Max $\dot{M}_{out}$

To calculate the maximum mass flow rate that can be pumped out of the chamber by the diffusion pump, the specific operating parameters of the pump must be defined. The SVF utilizes a Varian VHS-6 diffusion pump with pumping speed and capacity illustrated in the Speed Curve in Figure 33. The diffusion pump must be roughed down to its operation pressure conditions, below 10^{-2} Torr in order to run experiments at or below that pressure. If experimental conditions require pressure conditions above the operating range of the diffusion pump, then the roughing pump would be used to maintain these

conditions in the test chamber. Therefore, a Speed Curve of the mechanical pump is also provided in Figure 34.

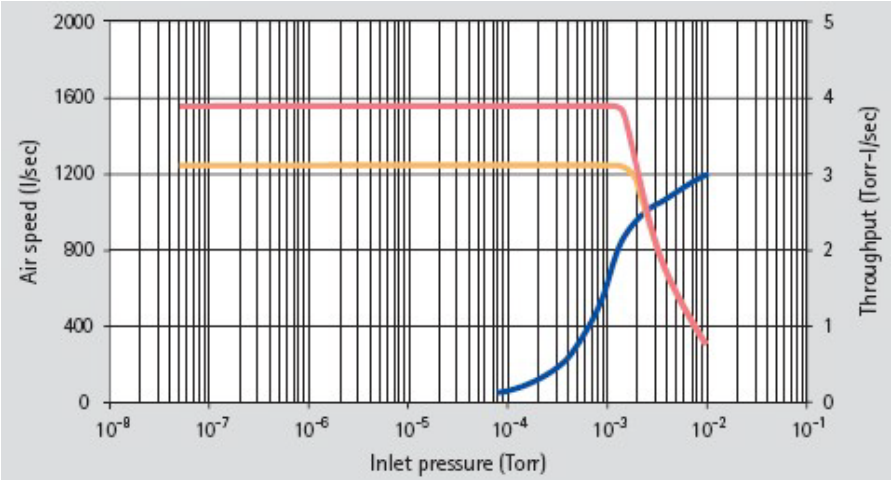

Figure 33: Speed Curve for Varian VHS-6 Diffusion Pump (VarianInc.com)

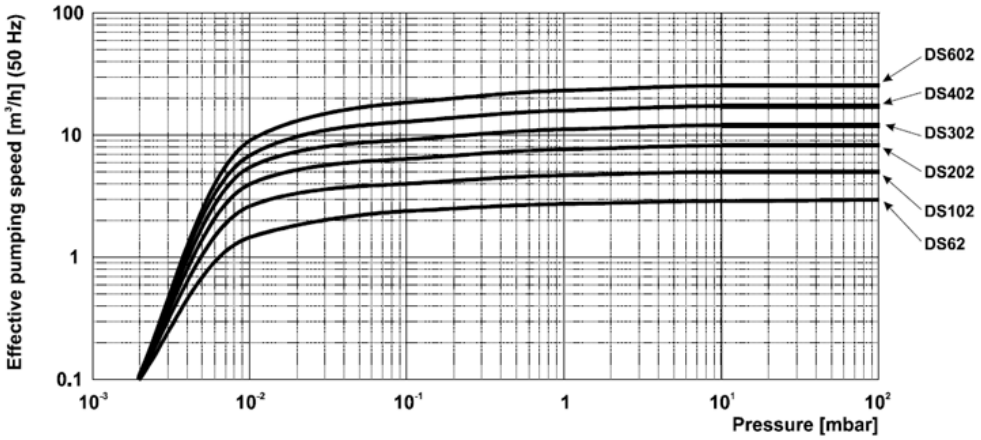

Figure 34: Speed Curve for DS602 3Ph Dual Stage Rotary Vane (Mechanical) Pump

From the pumps' speed curves, pumping speeds at given inlet pressures (background chamber pressures) can be obtained. The operating pumping speed in units of $\left[\frac{l}{s}\right]$ can be converted to volumetric flow rate, which is in units of $\left[\frac{l}{min}\right]$; this is simply so that it can be used in an Excel program (John J. Blandino, Appendix A). The Excel program uses this measurement to calculate the final maximum mass flow rate out of chamber by implementing testing conditions and the properties of nitrogen in a simple

conversion. In this Excel program, the inputs (in red) are the volumetric flow rate obtained from the speed curves as well as the testing conditions; the outputs are throughput and mass flow rate.

Table 3: Reservoir and Background Chamber Testing Condition

Reservoir Pressure		Reservoir Temp		Background Pressure		Background Temp	
14.70	psia	25.00	C	1.00E-03	torr	25.00	C
1.00	atm	298.15	K	1.32E-06	atm	298.15	K
101352.92	Pa	77.00	F	0.1333224	Pa	77.00	F

Table 4: Mass Flow Conversion Calculator

Calc mdot from S					
Vol. Flowrate:S	93000	l/min		Max Mdot out	
	1.55	m^3/sec	S T P	1.936321	kg/s
			Supply	1.774449	kg/s
Throughput* (Q)	1.55	Torr-l/s	Chamber	2.33E-06	kg/s

For the purpose of illustrating the conversion from volumetric flow rate to throughput and mass flow rate, the calculations performed by this Excel program are described in a series of steps. First, throughput is calculated from volumetric flow rate in units of $\left[\frac{l}{min}\right]$ using equation (3.2). Next the density of the gas, which is in units of $\left[\frac{kg}{m^3}\right]$ must be calculated inside the test chamber at the given conditions:

$$\rho = \frac{p_b}{R_{specific}\, T} \tag{3.38}$$

Using the calculated density, equation (3.38), mass flow rate $\left[\frac{kg}{s}\right]$ is obtained by converting volumetric flow rate into units of $\left[\frac{m^3}{s}\right]$ and multiplying by the flow density.

$$\dot{m} = S\rho = \frac{l}{min}\frac{m^3}{1000l}\frac{kg}{m^3}\frac{min}{3600s} \tag{3.39}$$

The calculated throughput can be compared to the throughput on the pump speed curve to confirm that the diffusion pump is operating at the stated capacity. In addition, the maximum mass flow rate that the pump can handle can be compared to the mass flow rate obtained from the original orifice

calculations. From the mass flow conversion calculator, the mass flow rate at the background chamber conditions given above is 2.33 X 10^{-6} [kg/s]. Incorporating the same conditions into the MATLAB and Excel code (with input background pressures) gives a range of mass flow rates as illustrated in the Figure 35 and Figure 36. It can be seen that the maximum mass flow rate achievable by the pump is at the upper limit of the plotted flow rates (calculated from orifice flow theory), which simply means that the facility can run at the desired testing conditions and orifice diameters. Plots were generated at different background pressures ranging from atmospheric pressure to vacuum pressure. Based on the operating range of the diffusion pump, (1.5 X 10^{-3} to 5.0 X 10^{-9} Torr), the upper limit of the mass flow rates achievable is shown in Figure 35. The lower limit of the mass flow rates is shown in Figure 36 with the only change being the pump flow limit decrease due to the change in background pressure. The upper limit of the mass flow rate achievable by the pump is signified on each plot by a blue horizontal line.

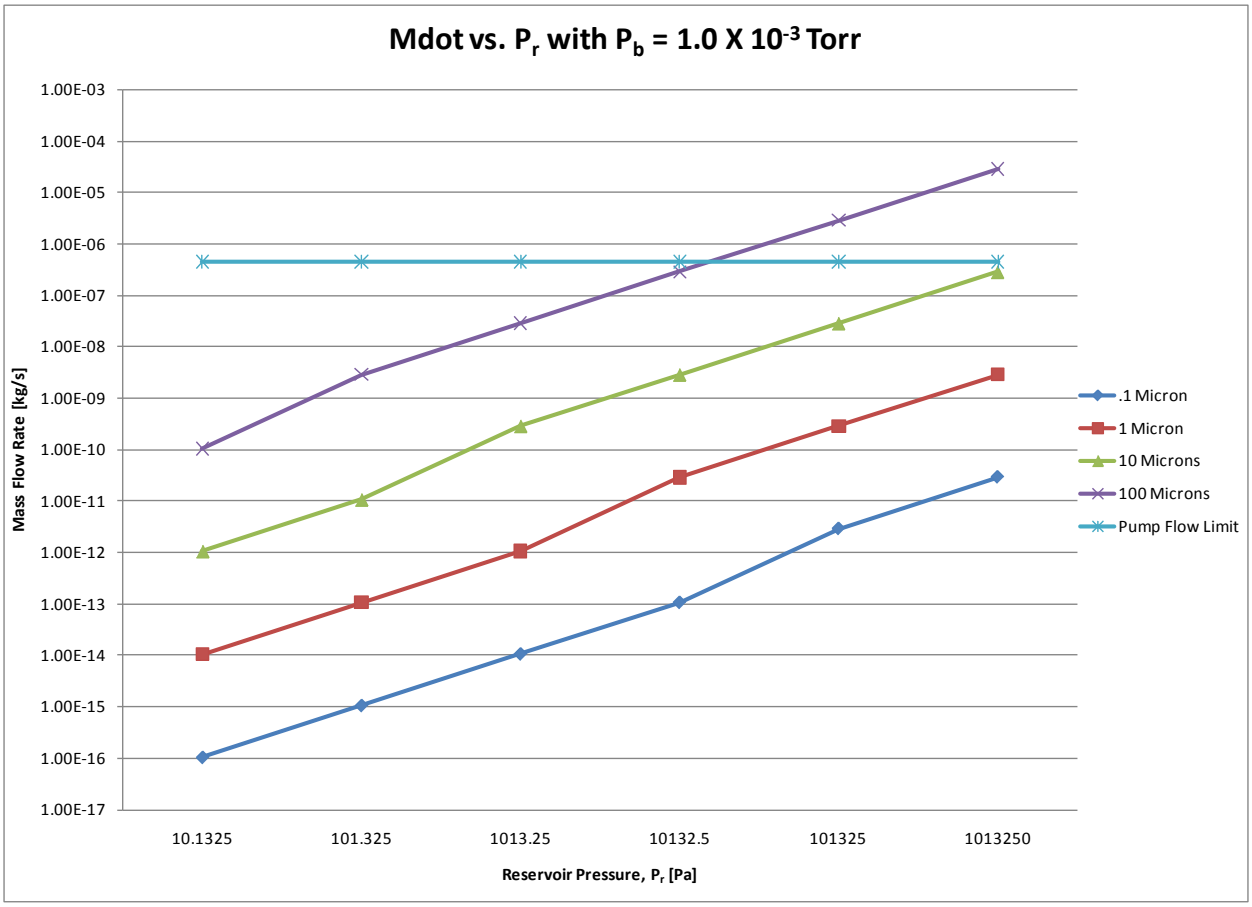

Figure 35: Mass Flow Rate versus P_r with P_b 1.0 X 10^{-3} Torr

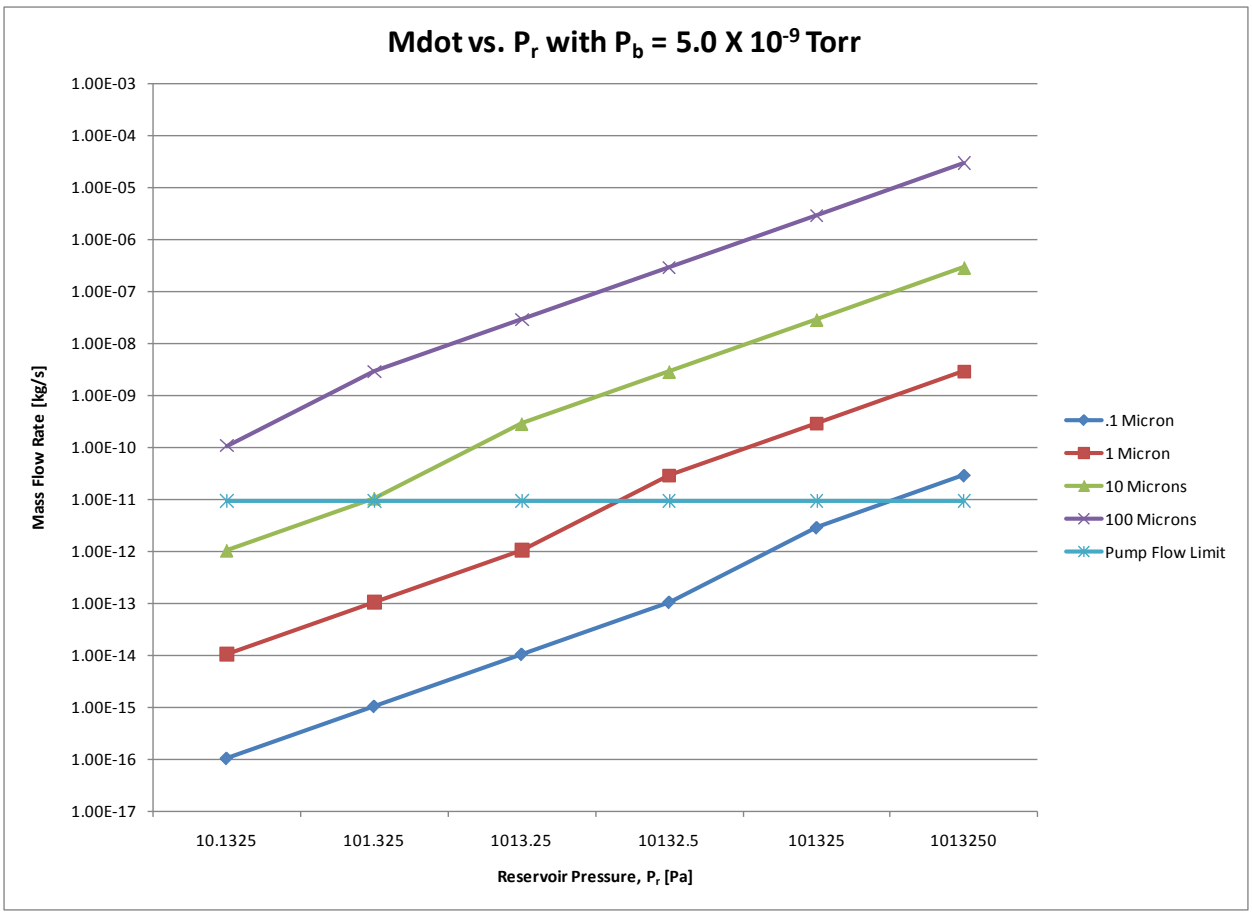

Figure 36: Mass Flow Rate versus P_r with P_b 5.0 X 10^{-9} Torr

4 – Summary and Recommendations

The goals achieved in this MQP are:

1. Integration of an automated hoist system with the support table of the SVF.
2. Analysis of free-molecular and continuum flows through 0.1 – 100 micron-diameter orifices into the 10^{-3} – 10^{-9} Torr bell-jar and throughput analysis of the SVF's diffusion pump.

4.1 Design and Integration of the Hoist System

An automated hoist that met the design and cost criteria was identified and procured. The integration process itself resulted in new design objectives for additional components: a support bracket to attach the hoist to the bell jar and a base plate to hold the hoist system on the table structure. As with many design projects, several constraints were encountered. One major constraint resulted from the requirement for accommodating the procured gate valve under the table. The design iterations resulted in positioning the hoist system to the short side of the support table and modifications to the table structure. These include the extension of the circular hole on the top surface of the table structure to a 0.1524 m (6 inches) cut to the left and the repositioning of the support bars beneath the top surface.

The design iterations were performed using Pro/E and Mechanica to ensure appropriate stresses and minimum deflections. The design accomplished a safety factor of more than 2 in stress-concentrated areas as well as minimal deformations and deflections in order of less than 0.001m (0.039in).

The fabrication of components and integration of the hoist with the support table are pursued with a commercial vendor identified by this MQP group.

Future work should be directed towards the integration of the control and electronics boards for the hoist and pumps of the SVF.

4.2 Microflow and Throughput Analysis

One of the main goals of this project is to examine operating conditions of the vacuum chamber to support testing of nitrogen microjets. These microjets will be produced by microtubes or micro-orifices placed inside the SVF's bell jar. The MQP obtained estimates of mass flow rates from orifices with diameters between 0.1 – 100 microns operating with reservoir pressures from 0.133 – 1.01325×10^{6} Pa into a background chamber with pressures from 10^{-3} – 5×10^{-9} Torr. The background pressures correspond to the Varian VHS-6 diffusion pump's operating range. The estimates are obtained using

theoretical models for free-molecular effusion and continuum flow through an orifice, implemented into MATLAB and Excel.

The throughput of the VHS-6 pump is used to ascertain the range of mass flow rates that can be pumped from the bell jar. Our analysis shows that for orifice diameters ranging from 0.1 to 100 microns, nearly all of the reservoir pressures considered result in mass flows in the bell jar within the acceptable pumping ability.

Future work must proceed with the implementation of models for tube flows and subsequently, the design and implementation of the flow delivery system.

References

Bird, G. A. *Monte Carlo Simulation of Gas Flow*. Tech. 11th ed. Vol. 10. Sydney, AU: Annual Review Inc., 1978. Print. Ser. 31.

Chamberlin, R., "A Three-dimensional Direct Simulation Monte Carlo Methodology on Unstructured Delaney Grids with Applications to Microflows and Nanoflows," Ph.D. Dissertation, WPI, March 2007.

Chamberlin, R.E. and Gatsonis, N.A., "Numerical Modeling of Gas Expansion from Microtubes," *Journal of Nanoscale and Microscale Thermophysical Engineering*, Vol. 12, No. 2, pp. 170-185, 2008.

Chamberlin, R. E., and Gatsonis, N. A., "DSMC Simulation of Microjet Expansion and the Design of a Micro Pitot Probe," AIAA- 2006 379, 9th AIAA Joint Thermophysics and Heat Transfer Conference, San Francisco, CA, June 2006.

Del Vecchio, Anthony, and Lawrence Loomis. "Design of Microflow Experiments." MQP. Worcester Polytechnic Institute, 2009.

Gombosi, Tamas. Gaskinetic Theory. Ch 4. New York: Cambridge University Press, 1994.

Heller, Jason, and Tim Padden. "A Microscale Mass-Flow Measuring System." MQP. Worcester Polytechnic Institute, 2006.

Herrera, Victor, Michael Macri, and Von Tourgee. "Integration of a Small Vacuum Facility." MQP. Worcester Polytechnic Institute, 2008.

Jahns, Jan. Mass Flow Through an Orifice. Retrieved November, 2009. From http://www.therebreathersite.nl/01_Informative/gas_flow_through_an_orifice.htm

John, James E.. Measurements in Compressible Flow. Chapter 15.6. "Flow Rate Measurement"

Lesker Company. Motorized Hoist & Accessories. Retrieved October 2009. From http://www.lesker.com/newweb/chambers/Motorized_Hoists.cfm

O'Hanlon, John F.. Users Guide to Vacuum Technology. John Wiley & Sons, Inc. 2005.

Varian Inc. Basic Vacuum Theory. 1992.

Appendix A: Flow Calculator Excel Program

2.0 FLOW CONVERSION

2.1 Supply and Chamber Pressure and Temp

Supply Pressure		Supply Temp		Chamber Pressure		Chamber Temp	
14.70	psia	25.00	C	2.25E-01	torr	25.00	C
1.00	atm	298.15	K	2.96E-04	atm	298.15	K
101352.92	Pa	77.00	F	29.997533	Pa	77.00	F

2.2 Gas Properties

Gas Const. 8314.34 J/kmol/k STP=1 atm, 0 C

GAS	MW (kg/kmol)	R (J/kg/K)	STP Density (kg/m^3)	Supply Density (kg/m^3)	Chamber Density (kg/m^3)
Argon	39.95	208.11865	1.782	1.633	0.0004834
Hydrogen	2.00	4157.17	0.089	0.082	2.42E-05
Air	28.80	288.69236	1.285	1.178	0.0003485
Xe	131.29	63.328052	5.858	5.368	0.0015887
Nitrogen	28.00	296.94071	1.249	1.145	0.0003388
Methane	16.00	519.64625	0.714	0.654	0.0001936
Water Vapor	18.00	461.90778	----	----	0.0002178

2.3 Mass-Volume Flow Conversion Calculator

Calc mdot from S

Vol. Flowrate:S	1.500E-03	l/min	mdot	Argon	Hydrogen	Air	Xe	Nitrogen	Methane	
	2.500E-08	m^3/sec	S T P	4.456E-05	2.231E-06	3.212E-05	1.464E-04	3.123E-05	1.785E-05	g/s
			Supply	4.083E-05	2.044E-06	2.944E-05	1.342E-04	2.862E-05	1.635E-05	g/s
Throughput* (Q)	5.625E-06	Torr-l/s	Chamber	1.209E-08	6.051E-10	8.713E-09	3.972E-08	8.471E-09	4.840E-09	g/s

Calc S from mdot

mdot	1.209E-08	g/s	Vol. Flowrate: S	Argon	Hydrogen	Air	Xe	Nitrogen	Methane	
	1.209E-11	kg/sec	S T P	4.070E-07	8.129E-06	5.645E-07	1.238E-07	5.807E-07	1.016E-06	l/min
			Supply	4.441E-07	8.871E-06	6.160E-07	1.351E-07	6.336E-07	1.109E-06	l/min
			Chamber	1.501E-03	2.997E-02	2.081E-03	4.566E-04	2.141E-03	3.747E-03	l/min
			Throughput (Q)	5.627E-06	1.124E-04	7.805E-06	1.712E-06	8.028E-06	1.405E-05	Torr-l/s

* Q calc assumes all gas is at chamber temp and pressure

2.4 Volume Flow Conversion Calculator

Cubic Meters per second	minute	hour	Liters per second	minute	hour	Cubic Feet per second	minute	hour	Cubic Centimeters pe second	minute
1	60	3600	1000	60000	3600000	35.31467	2118.8802	127132.81	1000000	60000000
0.016666667	1	60	16.66666667	1000	60000	0.5885778	35.31467	2118.8802	16666.667	1000000
0.000277778	0.0166667	1	0.277777778	16.666667	1000	0.0098096	0.5885778	35.31467	277.77778	16666.667
0.001	0.06	3.6	1	60	3600	0.0353147	2.1188802	127.13281	1000	60000
1.66667E-05	0.001	0.06	0.016666667	1	60	0.0005886	0.0353147	2.1188802	16.666667	1000
2.77778E-07	1.667E-05	0.001	0.000277778	0.0166667	1	9.81E-06	0.0005886	0.0353147	0.2777778	16.666667
0.02831685	1.699011	101.94066	28.31685	1699.011	101940.66	1	60	3600	28316.85	1699011
0.000471948	0.0283169	1.699011	0.4719475	28.31685	1699.011	0.0166667	1	60	471.9475	28316.85
7.86579E-06	0.0004719	0.0283169	0.007865792	0.4719475	28.31685	0.0002778	0.0166667	1	7.8657917	471.9475
0.000001	0.00006	0.0036	0.001	0.06	3.6	3.531E-05	0.0021189	0.1271328	1	60

Appendix B: Excel Mass Flow Program

Diameter	P1	Pb	Pc	gamma	R	T	k
1.00E-07	1013250	1.33E-01	534089.778	1.407	296.8	298.15	1.38E-23
	101325	1.33E-01	53408.9778				
	10132.5	1.33E-01	5340.89778				
	1013.25	1.33E-01	534.089778				
	101.325	1.33E-01	53.4089778				
	10.1325	1.33E-01	5.34089778				

dmol	m	n	lambda	kn	mdot
4.17E-10	4.65E-26	2.46265E+26	5.25606E-09	0.0525606	2.89243E-11
		2.46265E+25	5.25606E-08	0.52560599	2.89243E-12
		2.46265E+24	5.25606E-07	5.25605991	1.06728E-13
		2.46265E+23	5.25606E-06	52.5605991	1.06716E-14
		2.46265E+22	5.25606E-05	525.605991	1.0659E-15
		2.46265E+21	0.000525606	5256.05991	1.05329E-16

Orifice Diameter						Chamber				
1.00E-07	1.00E-06	1.00E-05	1.00E-04	Pr	Pb	Density	Volumetric flowrate		Throughput	Pump Mdotout
						[kg/m^3]	[l/s]	[m^3/s]	[Torr-l/s]	
2.89E-11	2.89E-09	2.89E-07	2.89E-05	1013250	101325					
0	0	0	0.00E+00	101325	101325					
-9.6E-13	#NUM!	#NUM!	#NUM!	10132.5	101325					
-1.1E-12	-1.1E-10	#NUM!	#NUM!	1013.25	101325					
-1.1E-12	-1.1E-10	-1.1E-08	#NUM!	101.325	101325					
-1.1E-12	-1.1E-10	-1.1E-08	-1.07E-06	10.1325	101325					
2.89E-11	2.89E-09	2.89E-07	2.89E-05	1013250	50662.5					
2.89E-12	2.89E-10	2.89E-08	2.89E-06	101325	50662.5					
-4.3E-13	#NUM!	#NUM!	#NUM!	10132.5	50662.5					
-5.2E-13	-5.2E-11	#NUM!	#NUM!	1013.25	50662.5					
-5.3E-13	-5.3E-11	-5.3E-09	#NUM!	101.325	50662.5					
-5.3E-13	-5.3E-11	-5.3E-09	-5.34E-07	10.1325	50662.5					
2.89E-11	2.89E-09	2.89E-07	2.89E-05	1013250	1.33E-01	1.50662E-06	300	0.3	3.000E-01	4.51987E-07
2.89E-12	2.89E-10	2.89E-08	2.89E-06	101325	1.33E-01	1.50662E-06	300	0.3	3.000E-01	4.51987E-07
1.07E-13	2.89E-11	2.89E-09	2.89E-07	10132.5	1.33E-01	1.50662E-06	300	0.3	3.000E-01	4.51987E-07
1.07E-14	1.07E-12	2.89E-10	2.89E-08	1013.25	1.33E-01	1.50662E-06	300	0.3	3.000E-01	4.51987E-07
1.07E-15	1.07E-13	1.07E-11	2.89E-09	101.325	1.33E-01	1.50662E-06	300	0.3	3.000E-01	4.51987E-07
1.05E-16	1.05E-14	1.05E-12	1.05E-10	10.1325	1.33E-01	1.50662E-06	300	0.3	3.000E-01	4.51987E-07
						0				
2.89E-11	2.89E-09	2.89E-07	2.89E-05	1013250	1.33E-02	1.50662E-07	1.25E+03	1.25	1.250E-01	1.88328E-07
2.89E-12	2.89E-10	2.89E-08	2.89E-06	101325	1.33E-02	1.50662E-07	1.25E+03	1.25	1.250E-01	1.88328E-07
1.07E-13	2.89E-11	2.89E-09	2.89E-07	10132.5	1.33E-02	1.50662E-07	1.25E+03	1.25	1.250E-01	1.88328E-07
1.07E-14	1.07E-12	2.89E-10	2.89E-08	1013.25	1.33E-02	1.50662E-07	1.25E+03	1.25	1.250E-01	1.88328E-07
1.07E-15	1.07E-13	1.07E-11	2.89E-09	101.325	1.33E-02	1.50662E-07	1.25E+03	1.25	1.250E-01	1.88328E-07
1.07E-16	1.07E-14	1.07E-12	1.07E-10	10.1325	1.33E-02	1.50662E-07	1.25E+03	1.25	1.250E-01	1.88328E-07
						0				
2.89E-11	2.89E-09	2.89E-07	2.89E-05	1013250	1.33E-03	1.50662E-08	1.25E+03	1.25	1.250E-02	1.88328E-08
2.89E-12	2.89E-10	2.89E-08	2.89E-06	101325	1.33E-03	1.50662E-08	1.25E+03	1.25	1.250E-02	1.88328E-08
1.07E-13	2.89E-11	2.89E-09	2.89E-07	10132.5	1.33E-03	1.50662E-08	1.25E+03	1.25	1.250E-02	1.88328E-08
1.07E-14	1.07E-12	2.89E-10	2.89E-08	1013.25	1.33E-03	1.50662E-08	1.25E+03	1.25	1.250E-02	1.88328E-08
1.07E-15	1.07E-13	1.07E-11	2.89E-09	101.325	1.33E-03	1.50662E-08	1.25E+03	1.25	1.250E-02	1.88328E-08
1.07E-16	1.07E-14	1.07E-12	1.07E-10	10.1325	1.33E-03	1.50662E-08	1.25E+03	1.25	1.250E-02	1.88328E-08
						0				
2.89E-11	2.89E-09	2.89E-07	2.89E-05	1013250	1.33E-05	1.50662E-10	1.25E+03	1.25	1.250E-04	1.88328E-10
2.89E-12	2.89E-10	2.89E-08	2.89E-06	101325	1.33E-05	1.50662E-10	1.25E+03	1.25	1.250E-04	1.88328E-10
1.07E-13	2.89E-11	2.89E-09	2.89E-07	10132.5	1.33E-05	1.50662E-10	1.25E+03	1.25	1.250E-04	1.88328E-10
1.07E-14	1.07E-12	2.89E-10	2.89E-08	1013.25	1.33E-05	1.50662E-10	1.25E+03	1.25	1.250E-04	1.88328E-10
1.07E-15	1.07E-13	1.07E-11	2.89E-09	101.325	1.33E-05	1.50662E-10	1.25E+03	1.25	1.250E-04	1.88328E-10
1.07E-16	1.07E-14	1.07E-12	1.07E-10	10.1325	1.33E-05	1.50662E-10	1.25E+03	1.25	1.250E-04	1.88328E-10
						0				
2.89E-11	2.89E-09	2.89E-07	2.89E-05	1013250	6.67E-07	7.53311E-12	1.25E+03	1.25	6.250E-06	9.41639E-12
2.89E-12	2.89E-10	2.89E-08	2.89E-06	101325	6.67E-07	7.53311E-12	1.25E+03	1.25	6.250E-06	9.41639E-12
1.07E-13	2.89E-11	2.89E-09	2.89E-07	10132.5	6.67E-07	7.53311E-12	1.25E+03	1.25	6.250E-06	9.41639E-12
1.07E-14	1.07E-12	2.89E-10	2.89E-08	1013.25	6.67E-07	7.53311E-12	1.25E+03	1.25	6.250E-06	9.41639E-12
1.07E-15	1.07E-13	1.07E-11	2.89E-09	101.325	6.67E-07	7.53311E-12	1.25E+03	1.25	6.250E-06	9.41639E-12
1.07E-16	1.07E-14	1.07E-12	1.07E-10	10.1325	6.67E-07	7.53311E-12	1.25E+03	1.25	6.250E-06	9.41639E-12

Appendix C: MATLAB Program (Created by MQP Team)

```
clear all
hold off
close all
clc


%% Parameters and Constants

% Constants
k=1.38*10^(-23); % Boltzmann Constant
r=296.8; % Specific Gas Constant for N2
mkg=46.5*10^(-27); %molecular mass of N2 in kg
dmol=4.17*10^(-10); %molecular diameter of N2 in meters
gamma=1.407; %specific heat ratio
pi=3.1415926535;
T1=300; %Kelvin
P1init=101325; %Pascals
d=[1 5 25 100].*10^-6; %diameter of opening in meters (1 to 100 microns)
p1=[1013.25 10132.5 101325 1013250]; %Reservoir Pressure, Pascals
pb=.133322; %Background Pressure, Pascals
m=28.013; %molecular mass, N2
%number density in reservoir 1, (.932 was used, now calculated below)
rho=1.251; %density of nitrogen grams/L

%%
for ii=1:length(d)
    for i=1:length(p1)
        n1(i)=p1(i)/(k*T1); %particles per cubic meter
        lambda(i)=1/(sqrt(2)*pi*dmol^2*n1(i));
        Kn(i,ii)=lambda(i)/d(ii);
    end
end

%hold on

%%
for i=1:length(p1); %test will run with 5 different pressures entered above
    for ii=1:length(d); %test runs every diameter of hole in microns for each
pressure
        for iii=1:length(n1);
            %Continuum
            if Kn(i,ii)<=1
                pcrit=p1(i)*(2/(gamma+1))^(gamma/(gamma-1)); %calculates the
critical pressure
                if pb<=pcrit
                    u=(((2*gamma)/(gamma+1))*(p1(i)/(m*n1(iii))))^(1/2);
%outflow velocity
                else
                    u=((2/(gamma-1))*((gamma*p1(i))/(m*n1(iii)))*(1-
(pb/p1(i))^((gamma-1)/gamma)))^.5; %outflow velocity u
                end
                rho=p1(i)/(r*T1);
                A=pi*(d(ii)/2)^2;
```

```
                mdot(i,ii)=(rho*u*A);

                %Rarified
            elseif Kn(i,ii)>1
                mdot(i,ii)=(pi*(d(ii)/2)^2)*(p1(i)-pb)/((m/(2*pi*k*T1))^.5);
            end
        end
    end
end

%%
figure(1)
loglog(p1,mdot)

if Kn(i,ii)<=1
    title({'Mdot v. Pressure w/ Pb=.001 Torr';'Continuum'})
elseif Kn(i,ii)>1
    title({'Mdot v. Pressure w/ Pb=.001 Torr';'Rarefied'})
end
xlabel('Pascals')
ylabel('Kg/sec')
legend('.1x10^-^6 m', '1x10^-^6 m', '10x10^-^6 m', '100x10^-^6 m', 2)
```

Appendix D: MATLAB Code (Created by Michael Morin)

```
clear all
hold off
close all

% Change only the Background Pressure Here
p2=.000000667;
%.....................................
p1=[10^-4,2.5*10^-4,5*10^-4,7.5*10^-4,10^-3,2.5*10^-3,5*10^-3,7.5*10^-3,10^-
2,2.5*10^-2,5*10^-2,7.5*10^-2,10^-1,2.5*10^-1,5*10^-1,7.5*10^-
1,1,2.5,5,7.5,10]*101325;
T=298.15; k=1.38*10^-23;
n2=p2/(k*T);
d=4.17*10^(-10); m=28.0134*10^-3/(6.0221415*10^23); gamma=1.407;
pi=3.1415926535;
D=[.1,1,10,100]*10^-6 ;

mdot=zeros(length(p1),length(D));
for j=1:length(p1)%iterate over pressure
    n1=p1(j)/(k*T);
    lambda=1/(sqrt(2)*pi*d^2*n1);
    for i=1:length(D)%iterate over diameter
        kn=lambda/D(i);
        area=pi*(D(i)/2)^2;
        flux=0;
        if (kn<=1) && (kn>0)
            a1=sqrt(gamma*p1(j)/(m*n1));
            pc=p1(j)*(2/(gamma+1))^(gamma/(gamma-1));
            if p2<=pc
                flux=n1*a1*(2/(gamma+1))^((gamma+1)/(2*(gamma-1)));
            else
                norf=n1*(p2/p1)^(1/gamma);
                uorf=a1*sqrt((2/(gamma-1))*(1-(p2/p1)^((gamma-1)/gamma)));
                flux=norf*uorf;
            end
        elseif kn>1
            flux=(n1-n2)*sqrt(k*T/(2*pi*m));
        end
        mdot(j,i)=flux*area*m;
    end
end

figure1=figure;
% Create axes
axes1 = axes('Parent',figure1,...
    'YTickLabel',{'10^-16','10^-15','10^-14','10^-13','10^-12','10^-11','10^-
10','10^-9','10^-8','10^-7','10^-6','10^-5'},...
    'YTick',[1e-016 1e-015 1e-014 1e-013 1e-012 1e-011 1e-010 1e-009 1e-008
1e-007 1e-006 1e-005],...
    'YScale','log',...
    'YMinorGrid','on',...
    'YGrid','on',...

'XTickLabel',{'10.1325','101.325','1013.25','10132.5','101325','1013250'},...
    'XTick',[10.1325 101.325 1013.25 10132.5 101325 1013250],...
```

```
    'XScale','log',...
    'XMinorTick','off',...
    'MinorGridLineStyle','none',...
    'GridLineStyle','--');
% Uncomment the following line to preserve the X-limits of the axes
 xlim(axes1,[5 1500000]);
% Uncomment the following line to preserve the Y-limits of the axes
 ylim(axes1,[1e-017 0.0001]);
box(axes1,'on');
hold(axes1,'all');

% Create multiple lines using matrix input to loglog
loglog(p1,mdot,'Parent',axes1);

% Create title
title(['Mdot v. Diameter w/ Pb = ', num2str(p2) , ' Torr']);

% Create xlabel
xlabel('Pa');

% Create ylabel
ylabel('Kg/Sec');
```